Detection of cracks in simply-supported beams by continuous wavelet transform of reconstructed modal data

Shuncong Zhong [1,2] and S Olutunde Oyadiji [3*]

1. School of Mechanical Engineering and Automation, Fuzhou University, 350108. P. R. China

2. Department of Electrical Engineering and Electronics, The University of Liverpool, Liverpool L69 3GJ, UK

3. Dynamics and Aeroelasticity Group, School of Mechanical, Aerospace and Civil Engineering, The University of Manchester, M13 9PL, UK

Abstract

This paper proposes a new approach for damage detection in beam-like structures with small cracks, whose crack ratio ($r = H_c / H$) is less than 5%, without baseline modal parameters. The approach is based on the difference of the Continuous Wavelet Transforms (CWTs) of two sets of mode shape data which correspond to the left half and the right half of the modal data of a cracked simply supported beam. The mode shape data of a cracked beam, are apparently smooth curves, but actually exhibit local peaks or discontinuities in the region of damage because they include additional response due to the cracks. The modal responses of the damaged simply-supported beams used are computed using the finite element method. The results demonstrate the efficiency of the proposed method for crack detection, and they provide a better crack indicator than the result of the CWT of the original mode shape data. The effects of

*Corresponding author. Tel: 00 44 161 275 4348 Fax: 00 44 161 275 3844
E-mail address: s.o.oyadiji@manchester.ac.uk (Dr. S O Oyadiji)

crack location and sampling interval are examined. The simulated and experimental results show that the proposed method has great potential in crack detection of beam-like structures as it does not require the modal parameter of an uncracked beam as a baseline for crack detection. It can be recommended for real applications.

Keywords

Beams, Crack Detection, Damage detection, Continuous Wavelet Transform, Modal data

1. Introduction

The interest in the ability to monitor a structure and detect damage at the earliest possible stage is pervasive throughout the civil, mechanical and aerospace engineering communities. During the past two decades, a variety of analytical, numerical and experimental investigations have been carried out on cracked structures with a view to developing robust crack detection methods. Any crack or localized damage in a structure reduces the stiffness and increases the damping in the structure. Reduction in stiffness is associated with decreases in the natural frequencies and modification of the mode shape of the structure. Several researchers have used mode shape measurements to detect damage. Pandey et al. [1] showed that absolute changes in the curvature mode shapes are localized in the region of damage and hence can be used to detect damage in a structure. The change in the curvature mode shapes increase with increasing size of damage. This information can be used to obtain the amount of damage in the structure. Ratcliffe [2] found that the mode shapes associated with higher natural frequencies can be used to verify the location of damage, but they are not as sensitive as the lower modes. Modal curvatures seem to be locally much more sensitive to damage than modal

displacements. In fact, the authors of this paper have shown that higher derivatives give a more sensitive detection [3]. Abdel Wahab and De Roeck [4] investigated the application of the change in modal curvatures to detect damage in a pre-stressed concrete bridge. They introduced a damage indicator called 'curvature damage factor'.

A crack in a structure introduces a local flexibility that can change the dynamic behaviour of the structure. Some damage index methods require the baseline data set of the intact structure for comparison to inspect the change in modal parameters due to damage. Typically, the baseline is obtained from measurements of the undamaged structure, As an example, Pandey et al. [1] compared the curvatures of the modes shapes between the undamaged and damaged structures. Sampaio et al. [5] directly subtracted the values of the mode shape curvature of the damaged structure from that of the undamaged structure.

In recent years, the use of wavelet analysis in damage detection has become an area of research activity in structural and machine health monitoring. The main advantage gained by using wavelets is the ability to perform local analysis of a signal which is capable of revealing some hidden aspects of the data that other signal analysis techniques fail to detect. This property is particularly important for damage detection applications. A review is provided by Peng and Chu [6] of available wavelet transformation methods and their application to machine condition monitoring. Deng and Wang [7] applied directly discrete wavelet transform to structural response signals to locate a crack along the length of a beam. Tian et al. [8] provided a method of crack detection in beams by wavelet analysis of transient flexural wave. Wang and Deng [9] discussed a structural damage detection technique based on wavelet analysis of spatially

distributed response measurements. The premise of the technique is that damage in a structure will cause structural response perturbations at damage sites. Such local perturbations, although they may not be apparent from the measured total response data, are often discernible from component wavelets. Liew and Wang [10] found that the presence of cracks can be detected by the change of some wavelet coefficients along the length of a structural component.

Gentile and Messina [11] were focused on the detection of open cracks in beam structures that undergo transverse vibrations. They used continuous wavelet transform to detect the location of open cracks in damaged beams by minimizing measurement data and baseline information of the structure. Quek et al. [12] examined the sensitivity of the wavelet technique in the detection of cracks in beam structure. Specially, the effects of different crack characteristics, boundary conditions, and wavelet functions used were investigated. Hong et al. [13] presented the effectiveness of the wavelet transform by means of its capability to estimate the Lipschitz exponent, whose magnitude can be used as a useful indicator of the damage extent. Damaged beams were investigated both numerically and experimentally. Yan et al. [14] evaluated the ability of detecting crack damage in a honeycomb sandwich plate by using natural frequency and dynamic response. They found energy spectrum of wavelet transform signals of structural dynamic response has higher sensitivity to crack damage. Douka et al. [15] used wavelet analysis for crack identification in beam structures. The fundamental vibration mode of a cracked cantilevered beam was analyzed using wavelet analysis and both the location and size of the crack are estimated.

Han et al. [16] proposed a damage detection index, which is called wavelet packet

energy rate index, for the damage detection of beam structures. The simulated and experimental studies demonstrated that the wavelet packet transform based energy rate index is a good candidate index that is sensitive to structural local damage. Chang and Chen [17] presented a technique for structure damage detection based on spatial wavelet analysis. Using the technique, the positions and depths of the cracks can be predicted with acceptable precision even though there are many cracks in the beam. Zumpano and Meo [18] presented a novel damage detection technique, tailored at the identification of structural surface damage on rail structures. The damage detection methodology developed was divided into three steps. The presence of the damage on the structure was assessed. In the second step, the arrival time of the reflected wave (or echo) was estimated using Continuous Wavelet Transform (CWT). Then, the detection algorithm was able, through a ray-tracing algorithm, to estimate the location of damage. Kim et al. [19] proposed a vibration-based damage evaluation method that can detect, locate, and size damage using multi-resolution wavelet analysis. Zhu and Law [20] presented a new method for crack identification of bridge beam structures under a moving load based on wavelet analysis. The proposed method is validated by both simulation and experiment. Locations of multiple damages can be located accurately, and the results are not sensitive to measurement noise, speed and magnitude of moving load, measuring location, etc.

This paper is aimed at detecting and locating cracks in damaged beams with small cracks, whose crack ratio is less than 5%. As stated in the previous paragraph, the minimum value of crack ratios using existing methods of crack detection is 5%. Even then, the existing methods only provide clear crack detection at crack ratio of 20% or greater. The aim of the present work is to develop a baseline-free method that will give

clear crack identification at crack ratios as small as 5% and even smaller. This new approach is based on finding the difference of the CWTs of the two sets of mode shape data. Those two modal data sets, which constitute two new signal series, are obtained and reconstructed from the modal displacement data of a cracked simply-supported beam. They represent the left half and the modified right half of the modal data of the simply supported beam. The left half of the modal data is the left half segment of the original mode shape data. For a symmetric mode shape, the modified right half modal data is obtained from rotating the right half segment of the mode shape about the vertical axis which passes through the centre of the mode shape, that is the vertical centre of the beam. For an antisymmetric mode shape, the modified right half segment is produced by rotating the right half of the mode shape twice: firstly about the vertical axis and secondly about the horizontal axis which pass through the centre of the mode shape.

CWT algorithm is firstly introduced in this paper. Then, a numerical example is provided to illustrate the operation of the method. This partly involves the computations of the first few natural frequencies and mode shapes of cracked simply supported beams using the ABAQUS finite element code. For brevity, only CWT of the first four mode shapes is investigated. The original mode shape data or 'signal' is divided and reconstructed into two signal series; one is the first half of the original mode shape 'signal', the other is a modified signal obtained from the second half of the original mode shape 'signal'. To further verify the efficiency and practicability of the proposed method, the effects of crack location, mode shape data sampling interval are investigated. The simulated and experimental results show that the proposed method has great potential in the field of crack detection of beam-like structures and can be

recommended for real applications.

2. Continuous wavelet transform

This section presents a brief background on continuous wavelet transform utilized in this paper. More facts on continuous wavelet transform can be found in the study of Daubechies [21].

A mother wavelet $\psi(x)$ can be defined as a function with zero average value,

$$\int_{-\infty}^{+\infty}\psi(x)dx = 0 \tag{1}$$

$\psi(x)$ is normalized:

$$\int_{-\infty}^{+\infty}\left|\psi(x)\right|^2 dx = 1 \tag{2}$$

From mother wavelet $\psi(x)$, the analyzing wavelets can be obtained by dilation parameter s and translation parameter b:

$$\psi_{b,s}(x) = \frac{1}{\sqrt{s}}\psi(\frac{x-b}{s}) \tag{3}$$

where both s and b are real numbers, and s must be positive.

The continuous wavelet transform of a signal $f(x) \in L^2(R)$ depending on time or space, is defined by

$$(Wf)(s,b) = \int_{-\infty}^{+\infty} f(x)\frac{1}{\sqrt{s}}\psi^*(\frac{x-b}{s})dx \tag{4}$$

where (*) denotes the complex conjugate, the mother wavelet should satisfy an admissibility condition to ensure existence of the inverse wavelet transform, such as

$$C_\psi = \int_{-\infty}^{+\infty} \frac{\left|F_\psi(\omega)\right|^2}{|\omega|} d\omega < \infty \tag{5}$$

where $F_\psi(\omega)$ denotes the Fourier transform of $\psi(x)$ defined as

$$F_\psi(\omega) = \int_{-\infty}^{+\infty} \psi(x) e^{-i\omega x} dx, \quad x \in R \tag{6}$$

The signal $f(x)$ may be recovered or reconstructed by an inverse wavelet transform of $Wf(s,b)$ defined as

$$f(x) = \frac{1}{C_\psi} \int_{-\infty}^{+\infty} \int_{-\infty}^{+\infty} (Wf)(s,b) \psi\left(\frac{x-b}{s}\right) \frac{dsdb}{s^2} \tag{7}$$

Also, the CWT may as well be performed in Fourier space [22]

$$(Wf)(s,b) = \frac{1}{2\pi} \int_{-\infty}^{+\infty} F_f(\omega) e^{ib\omega} F_\psi{}^*(s\omega) d\omega \tag{8}$$

where $F_f(\omega)$ is the Fourier transform of $f(x)$ defined as

$$F_f(\omega) = \int_{-\infty}^{+\infty} f(x) e^{-i\omega x} dx, \quad x \in R \tag{9}$$

The local resolution of the CWT in time or space and in frequency depends on the dilation parameter s and is determined, respectively, by the duration Δx_ψ and bandwidth $\Delta \omega_\psi$ of the mother wavelet [23] :

$$\Delta x = s\Delta x_{\psi}, \quad \Delta\omega = \frac{\Delta\omega_{\psi}}{s} \tag{10}$$

Here, Δx_{ψ} and $\Delta\omega_{\psi}$ are defined as

$$\Delta x_{\psi} = \frac{1}{\|\psi(x)\|_2}\sqrt{\int_{-\infty}^{+\infty}(x-x_{\psi})^2|\psi(x)|^2 dx} \tag{11}$$

$$\Delta\omega_{\psi} = \frac{1}{\|F_{\psi}(\omega)\|_2}\sqrt{\int_{-\infty}^{+\infty}(\omega-\omega_{\psi})^2|F_{\psi}(\omega)|^2 d\omega} \tag{12}$$

where x_{ψ} and ω_{ψ} are the centre of $\psi(x)$ and $F_{\psi}(\omega)$, respectively,

$$x_{\psi} = \int_{-\infty}^{+\infty} x\frac{|\psi(x)|^2}{\|\psi(x)\|_2^2}dx \tag{13}$$

$$\omega_{\psi} = \int_{-\infty}^{+\infty} \omega\frac{|F_{\psi}(\omega)|^2}{\|F_{\psi}(\omega)\|_2^2}d\omega \tag{14}$$

$\|\cdot\|_2$ denotes the classical norm in the space of square integrable functions.

It is well known that the number of vanishing moments is one of the most important factors for the success of wavelets in various applications [24]. In the present work, a symlet wavelet 'symmetrical 4' having four vanishing moments has been selected and used as the analyzing wavelet. The scaling function and wavelet function of 'symmetrical 4' wavelet are shown in Fig.1 (a) and (b).

3. Continuous wavelet transform of reconstructed mode shape data

The aim of the proposed method is to magnify small crack effects to make the crack

detectable when the cracks are in the early state. This method uses the difference of the CWTs of two reconstructed sets of data or signal series obtained from the original mode shape of a cracked beam. Firstly, the original mode shape signal is divided and reconstructed into two signal series as follows. If the original mode shape 'signal' is made up of $d_1, d_2, ..., d_N$ data points, where N is the total number of sampling points, the first segment ($s_1^{'}$) of the signal is the first half of the original mode shape 'signal', that is, $d_1, d_2, ...d_{N/2+1}$. The second segment ($s_2^{'}$) of the signal is the second half of the original mode shape 'signal', that is, $d_{N/2+1}, d_{N/2+2}, ..., d_N$. This process of dividing and reconstituting the signals is illustrated in Fig.2 (a-1) and (a-2) for modes 1 and 2, respectively, of the beam. There are two cases, namely symmetric and antisymmetric cases. For symmetric cases, the mode shape is symmetrical about the centre of the beam, as illustrated in Fig.2 (a-1) for the first mode. In this case, the modal data is cut into left and right segments $s_1^{'}$ and $s_2^{'}$, respectively. The right modal data segment is rotated about a vertical axis to produce a modified data set s_2 which is similar to the left modal data segment s_1. The two new signal series s_1 and s_2 are obtained as $d_1, d_2, ..., d_{N/2+1}$ (the signal series s_1) and $d_N, d_{N-1}, ..., d_{N/2+1}$ (the signal series s_2), as shown in Fig.2 (b-1). For antisymmetric cases, the mode shape is antisymmetrical about the centre of the beam as illustrated in Fig.2 (a-2) for the second mode. In this case, the right data segment is rotated twice: firstly about the vertical axis and secondly about the horizontal axis to produce a modified data set s_2. Thus, the two signal series will be $d_1, d_2, ..., d_{N/2+1}$ (the signal series s_1) and $-d_N, -d_{N-1}, ..., -d_{N/2+1}$ (the signal series s_2), as shown in Fig.2 (b-2).

Then the wavelet coefficients, the difference of CWT of s_1 and s_2, will be obtained after CWTs of s_1 and s_2 are performed. For the case of a beam with small cracks, CWT of s_1 or s_2 includes some crack information. However, due to the smallness of the crack, the distortion of the transformed data caused by the crack is not very significant and, therefore, can not provide a clear crack detection. Finally, the difference of the CWT of s_1 and s_2 is determined to give a better crack indication than the CWT of the original mode shape. However, it is noted that the proposed method is only suitable for the simply supported beams with symmetric and antisymmetric mode shapes.

4. Numerical example

4.1 Finite element modal analysis

In order to illustrate the applicability of the proposed method for crack detection, the natural frequencies and mode shapes of simply-supported cracked beams are computed using the ABAQUS finite element code. A simply supported beam with a single-sided transverse crack with a fixed depth H_c, a crack width W_c, and located at distance l_c from the left support is shown in Fig.3. A mild steel beam of breadth b =100 mm, depth H =25 mm and length L =3000 mm was modeled using 20 node 3D brick element which is denoted in the ABAQUS FE package as C3D20R. The material properties of the beam are: Young's modulus $E = 210GPa$, Density $\rho = 7850Kg/m^3$, Poisson's ratio $v = 0.3$. In the FE model, the axial length of elements used in the analysis was l_e = 5mm for a 3000 mm long cracked beam when the elements are not near the crack location, but a more refined mesh size ($l_e^{'}$ = 0.5mm) used near the crack

location as shown in Fig.4. The first 50 natural frequencies and mode shapes of damaged and intact beams are computed.

The cracks are 0.1 mm wide and 1 mm deep and are located at 500 mm, 1000 mm, 1500 mm, 2000 mm and 2500 mm from the left end of the beam. The crack ratio of all the beams is 4%. Three sampling distances of the mode shape data are studied, namely, x_s = 5, 25 and 50 mm. For the case of sampling distance 5 mm, the modal displacement data is sampled (from the top beam surface) at 5 mm interval along the lengths of the beams resulting in a total of 601 data points. But this represents too much measurement. Therefore, the cases of sampling distances of 25 mm and 50 mm, which are closer to real applications, are also studied.

4.2 Comparison of CWT of original mode shape data with difference of CWTs

The method proposed in the present work is compared with the method using CWT of the original mode shapes in the following part of this section. Fig.5 (a) to (d) show the wavelet coefficients of the original first, second, third and fourth mode shapes of the damaged beam with the crack located at 500 mm from the left end of the beam, and for a sampling distance of 5 mm. Four scales were used for analysis, namely: s = 5, 15, 25 and 35.

For modes 1 to 3, Fig. 5(a) to (c) provide obvious (unambiguous) evidence of crack existence at 500 mm from the left end of the cracked beam only when the wavelet scale is equal to or greater than 25 (i.e. s ≥ 25). But when s < 25, the figures do not provide very obvious evidence of crack existence. In fact, for mode 4, Fig.5 (d) shows very little discontinuity in the mode shape at the crack location.

Fig.6 (a) to (d) show the difference of the wavelet coefficients of s_1 and s_2 obtained from the first, second, third and fourth mode shape 'signals', respectively, of the damaged beam. All the figures provide evidence of crack existence at 500 mm from the left end of the beam because all the wavelet coefficients exhibit high peak values at this position. The results of the proposed method give better crack indication than those of the method using the CWT of the original mode shape data shown in Fig.5.

To be certain about the presence of the crack, however, one has to examine in detail the behaviours of the wavelet maxima at these points as the scale increases. Fig. 7 presents 3D and contour plots of the CWT coefficients of the original mode shape data for scales 1 – 48 of the first four mode shape data. It is seen that none of the figures clearly identifies the crack and its location.

Fig.8 (a-1) to (d-1) are the 3D plots of the difference of the CWT coefficients of the two signal series s_1 and s_2 for the first four mode shape data of the damaged beam. Similarly, Fig.8 (a-2) to (d-2) are the contour plots of the difference of the CWT coefficients of the two signal series s_1 and s_2. The figures show very clear evidences of crack existence at 500 mm.

It can be seen from Fig.8 that the absolute value of the modified wavelet maxima increases in a regular manner with increasing scale. Also, the absolute value of the wavelet maxima of higher mode shape data is greater than that of lower mode shape data. Comparing all the figures in Fig.7 and Fig.8, an important conclusion can be obtained that the difference of the CWT coefficients of s_1 and s_2 gives better crack indication than the CWT coefficients of the original mode shape data. Furthermore, the

wavelet maxima of higher original mode shape is also greater than that of lower original mode shape. In fact, the increase in magnitude of the coefficients for original mode shape and difference of mode shape is due to the fact that damage induced local response is easy to be captured by the higher modes [25]. Typically, damage is a local phenomenon. Local response is captured by higher frequency modes whereas lower frequency modes tend to capture the global response of the structure and are less sensitive to local changes in a structure [26].

5. Further verification of the proposed method in crack detection

To verify the efficiency and practicability of the proposed method, a further 15 cases with cracks of varying location and using different sampling distances, as shown in Table 1, are studied. In this section, the effects of crack location and spatial intervals (sampling distances) of mode shape data on the difference of continuous wavelet transform (CWT) coefficients of the new signal series s_1 and s_2 are investigated.

5.1 Effect of crack location

Fig.9 (a-1) to (d-1) are, respectively, the 3D plots of the difference of the CWT coefficients of the two signal series s_1 and s_2 obtained from the first, second, third and fourth mode shape data of the damaged beam with the crack located at l_c = 1000 mm.

Fig.9 (a-2) to (d-2) show the corresponding contour plots of the difference of the CWT coefficients of the two signal series s_1 and s_2 obtained from the first four mode shape data of the damaged beam. There are obvious evidences of crack existence at location l_c = 1000 mm. Similar to the result given before, the absolute value of the

wavelet difference maxima increases in a regular manner with increasing scale. Also, the absolute value of the wavelet difference maxima of higher mode shape data is greater than that of lower mode shape data. The absolute value of the wavelet difference maxima of the first mode shape for the case of a crack located at 1000 mm is greater than that of the case of a crack located at 500 mm. However, the absolute value of the wavelet difference maxima of the second mode shape for the case of a crack located at 1000 mm is equal to that of the case of a crack located at 500 mm. The reason is that the modal displacements of points far away from the node of a mode are greater than those of points close to the node of the mode. Thus, in the case of mode 1, the CWT at 1000 mm is greater than that at 500 mm because location l_c = 1000 mm is further away from a node than location l_c = 500 mm. But in the case of mode 2, the CWT at 1000 mm is equal to that at 500 mm because locations l_c = 1000 mm and l_c = 500 mm are equidistant from the nodes of the mode shape of mode 2. For mode 3, the crack location is the node of the mode, therefore, the modal displacement for this case is close to zero, as shown in Fig.9 (c-1) and (c-2).

All the above discussion is focused on cracks located at the left part of the beam. A crack located at the right part of the beam is also investigated. Fig.10 (a-1) to (d-1) are, respectively, the 3D plots of the difference of the CWT coefficients of the two signal series s_1 and s_2 obtained from the first four mode shape data of the damaged beam with a crack located at 2000 mm from the left end of the beam. Fig.10 (a-2) to (d-2) show the corresponding contour plots of the difference of the CWT coefficients of the two signal series s_1 and s_2 for the first four mode shapes of the damaged beam. Except Fig.10 (c-1) and (c-2), the case of the crack located at the node of the third mode,

all the other figures indicate discontinuities at location 1000 mm which suggest the presence of a crack at this location. However, this is a pseudo location. The real location is at 2000 mm which is the mirror image of location 1000 mm. Also, in this case, the wavelet difference maxima are negative. However, the conclusion is still that the absolute value of the wavelet difference maxima increases in a regular manner with increasing scale. Furthermore, the absolute value of the wavelet maxima of higher mode shape data is greater than that of lower mode shape data.

When the crack is located at 2500 mm from the left end of the damaged beam, the 3D plots of the difference of the CWT coefficients of the two signal series s_1 and s_2 obtained from the first four mode shape data are shown in Fig.11 (a-1) to (d-1), respectively, while Fig.11 (a-2) to (d-2) show the corresponding contour plots of the difference of the CWT coefficients. These figures clearly indicate the presence of a crack at location 500 mm which is the mirror image of the actual location. Comparing Fig 11 (a-1) to (d-1) with Fig 8(a-1) to (d-1), respectively, it is seen that when the crack is located at l_c = 500 mm, the maxima of the difference of the CWT coefficient is positive. But when the crack is located at l_c = 2500 mm, the maxima of the difference of the CWT coefficient is negative. Therefore, the sign of the maxima of the difference of the CWT coefficient can be used to identify whether a crack is located on the left or right half of the simply-supported beam.

From the above discussion, it may be construed that the proposed method can only give good crack indication when the crack is not located at the centre of a beam. A legitimate question may be posed as to whether the proposed method is suitable for the special case of a crack located at the centre of beams. This problem is verified in the following.

A beam with a crack located at 1500 mm (the beam centre) from the left end of the beam, whose width and depth are 0.1 mm and 1 mm, respectively, is considered. The other parameters are the same as for the beams discussed previously. The original mode shapes are sampled at 5 mm interval along the lengths of the beams. Fig.12 (a-1) to (d-1) show the 3D plots of the difference of the CWT coefficients of the two signal series s_1 and s_2 obtained from the first four mode shape data. The corresponding contour plots of the difference of the CWT coefficients are shown in Fig.12 (a-2) to (d-2). It can be seen from Fig.12 (a-1), (a-2), (c-1) and (c-2) that there is no crack information manifested in the difference of the CWT transform coefficient of the two signal series s_1 and s_2 obtained from the first and third mode shapes. However, Fig.12 (b-1), (b-2), (d-1) and (d-2) show that the difference of the CWT coefficients for the second and fourth mode shapes indicates the presence of crack near the middle of the beam.

The principle of the proposed method results in the above observation which is summarized in the following. The first mode shape of a cracked simply-supported beam is a symmetrical one, and the two new signal series s_1 $(d_1, d_2, ..., d_{N/2+1})$ and s_2 $(d_N, d_{N-1}, ..., d_{N/2+1})$ are almost the same. Consequently, the difference between the CWT coefficient of s_1 and s_2 obtained from the first mode shape is very small. As for the second mode shape of a cracked simply-supported beam, it is an antisymmetrical one; the two new signal series s_1 $(d_1, d_2, ..., d_{N/2+1})$ and s_2 $(-d_N, -d_{N-1}, ..., -d_{N/2+1})$ have some difference in the cracked area. Hence, the difference of the CWT coefficients of s_1 and s_2 obtained from the second mode shape can give some crack information. The results can be seen from Fig.12 (b-1), and (b-2), which give obvious peak in the cracked area or its neighborhood. It can be seen that the magnitude of the difference of

the CWT coefficients of the second mode shape is very small being of the order of 10^{-8}. However, all the previous figures show that for a crack located away from the centre, the magnitude of the CWT coefficient difference is much greater than 10^{-8}. The reason for the very small magnitude of the CWT coefficient difference when the crack is located at the centre of the beam is due to the fact that the modal displacements of the second mode shape near the centre are very small in magnitude because the centre of the beam is a node for mode 2 of vibration. This results in the difference of the CWT coefficients of s_1 and s_2 obtained from the second mode shape being also small in magnitude. Nevertheless, the difference of the CWT coefficient of the second mode shape can still give crack information for damage detection.

Similarly, it was observed that the CWT coefficient difference of the third mode shape data gave no crack information whereas the CWT coefficient difference of the fourth mode shape data gave crack information. Thus, it can be generalized that when a crack is located at the centre of a simply-supported beam, the difference of the CWT coefficient of the symmetrical mode shapes will not provide crack information; only the difference of the CWT coefficient of the antisymmetrical mode shapes will provide crack information.

5.2 Effect of sampling distance

The results presented in the previous section were based on a sampling interval (distance) of the mode shape data of 5 mm. When the modal displacement data are sampled at distance intervals of 25 mm along the length of the beams, it results in a total of 121 data points.

In Fig.13 (a-1) to (d-1) are shown the 3D plots of the difference of the CWT coefficients of the two signal series s_1 and s_2 obtained from the first four mode shape data of the same damaged beam. The sampling distance is 25 mm. Fig.13 (a-2) to (d-2) are, respectively, the corresponding contour plots. The results clearly indicate the presence of a crack at the correct location of 500 mm.

A larger sampling distance of 50 mm was also investigated. Fig.14 (a-1) to (d-1) are, respectively, the 3D plots of the difference of the CWT coefficients of the two signal series s_1 and s_2 obtained from the first four mode shape data of the same damaged beam. The corresponding contour plots of the difference of the CWT coefficients of the two signal series s_1 and s_2 are shown in Fig.14 (a-2) to (d-2). The figures show that the accuracy of the crack location degrades as the sampling distance is increased. However, the difference of the CWT coefficient still gives reasonable information to enable crack detection.

5.3 Modified approach for real applications using large sampling distance

As discussed previously, the number of sensors available will be limited. This will result in large sampling distances. However, the accuracy of the detection of the crack location degrades as the sampling distance is increased. A larger sampling distance of 75 mm, which gives a total of 41 measurement points, was investigated.

Fig.15 (a-1) to (d-1) are, respectively, the 3D plots of the difference of the CWT coefficients of the two signal series s_1 and s_2 obtained from the first four mode shape data of the same damaged beam. The corresponding contour plots of the difference of the CWT coefficients of the two signal series s_1 and s_2 are shown in

Fig.15 (a-2) to (d-2). Similar to the results using smaller sampling distance (i.e. x_s = 50, 25, and 5 mm), the accuracy of the crack location degrades as the sampling distance is increased.

Now, in order to increase the accuracy of crack detection, before performing a CWT of the modal data, a spline interpolation is used for the mode shapes which are obtained using large sampling distances. Subsequently, the difference of the CWT coefficient of the two signal series s_1 and s_2 which are obtained from the interpolated mode shape data, is calculated as a damage indicator. The interpolation method can also be found in the studies of Wang and Deng [9] and Douka et al. [15].

A spline interpolation was applied to each set of 41 measured data points for the first two mode shapes. The interpolation step was 5 mm, resulting in a total number of 601 derived data points. Fig.16 (a-1) to (d-1) are, respectively, the 3D plots of CWT coefficients of the first four interpolated mode shape data. Fig.16 (a-2) to (d-2) are, respectively, the contour plots of the CWT coefficients of the first four interpolated mode shape data. However, all figures in Fig.16 do not clearly identify the crack nor its location. Therefore, using only the CWT of the original interpolated mode data can not provide clear crack indication for small cracks (crack ratio less than 5%) even if the original modal data is interpolated.

Fig.17 (a-1) to (d-1) are, respectively, the 3D plots of the difference of the CWT coefficients of the two signal series s_1 and s_2 obtained from the first four interpolated mode shape data of the damaged beam whose crack depth and width are 1 mm and 0.1 mm. The corresponding contour plots of the difference are shown in Fig.17 (a-2) to (d-2). The figures show very clear evidences of crack existence at 500 mm.

Comparing all the figures in Fig.16 and Fig.17, an important conclusion can be obtained that the modified approach gives better crack indication than the method using the CWT of the interpolated mode shape data, especially, when the crack ratio is relatively small (i.e. less than 5%) and the crack effect is small. Also, it can be seen from the figures in Fig.15 and Fig.17 that the accuracy of the crack detection increases dramatically after a spline interpolation is used for the mode shapes.

6. Experimental verification of the proposed method in crack detection

Experimental tests using a simply-supported aluminum beam were conducted. The dimensions of the damaged beam are $L \times H \times B = 2400 \times 25 \times 100 mm^3$. A crack, whose depth is 2.5mm, was located at $l_c = 0.4m$. Fig.18 shows the experimental set-up used for testing. A random signal was generated and then amplified by a power amplifier, and exerted on the beam structure through a shaker. The response signal and input signal were respectively sensed by a PCB (PCB Piezotronics, Inc.) accelerometer and a PCB force sensor. The displacement data is sampled at 100 mm ($x_s = 100\ mm$) interval along the lengths of the beam resulting in a total of 25 data points. Fig.19 shows the first four normalized measured mode shapes of the cracked beam.

A spline interpolation was applied to each set of 25 measured data points for the first four mode shapes. The interpolation step was 2 mm, resulting in a total number of 1201 derived data points. Fig.20 (a-1), (b-1), (c-1) and (d-1) show the 3D plots of the difference of the CWT coefficient of the two signal series s_1 and s_2 obtained from the first four interpolated mode shape data of the cracked aluminum beam. The corresponding contour plots of the difference are shown in Fig. 20 (a-2), (b-2), (c-2) and (d-2).

From the figures for mode 1 and mode 4, Fig.20 (a-1), (a-2), (d-1) and (d-2), it is seen that a crack is clearly located at 400 mm from the left end. However, from the figures for mode 2 and mode 3, due to the experimental noise effect, it is hard to determine the location of the crack though a peak appears at 400 mm from the left end. To improve the quality of the results, a simple denoising algorithm was employed: only wavelet coefficients of value more than 50% of the maximum value are considered. In other words, a threshold equal to 0.5 of the maximum value has been utilized [15]. The value of the wavelet coefficient is set to zero if it is less than 50% of maximum value, whilst the value of the wavelet coefficient is set to the difference between the wavelet coefficient and 50% of the maximum value if it is greater than 50% of maximum value. Symbolically, this is expressed as,

$$c' = \begin{cases} c - 0.5\hat{c}, & c > 0.5\hat{c} \\ 0, & c \le 0.5\hat{c} \end{cases} \tag{15}$$

where c, c' and $\hat{c}$ are the original, modified and maximum values of the wavelet coefficient respectively. It should be noted that this simple algorithm is similar to but different from the hard-thresholding function used in previous work [27-29].

Fig.21 (a-1 to (d-1) show the 3D plots of the difference of the CWT coefficients whose values are greater than 50% of the maximum value. The corresponding contour plots of the difference are shown in Fig. 21 (a-2) to (d-2). It can be seen from Fig.21 (a-1), (a-2), (d-1) and (d-2) that the improved results show very clear evidences of crack existence at 400 mm because all the wavelet coefficients exhibit high peak values at this position. However, for the mode 2, Fig.21 (b-1) and (b-2) show two almost equivalent peaks at 400 mm and 600 mm. Therefore, it is hard to make the decision where the crack is

located. Furthermore, for the mode 3, Fig.21 (c-1) and (c-2) show the wrong crack location at 600 mm due to the experimental noise. Here, one conclusion can be obtained that crack detection cannot only rely on the parameter of one single mode in the real applications because it is hard to distinguish the crack effect and the noise effect. More modal parameters should be considered simultaneously.

Secondly, to improve the results further, the number of spatial measurements should be increased substantially. It was not possible to carry out more measurements in the present work. Thirdly, in order to reduce the experimental noise effect, the following equation is proposed to be used as damage index for small crack detection in real applications,

$$\overline{A_d} = \frac{1}{N}\sum_{r=1}^{N} d_r \tag{16}$$

where d_r is the difference of the CWT coefficient of the two signal series s_1 and s_2 obtained from the mode shape for mode r, N is the number of mode shapes considered, $\overline{A}_d$ is the average of the difference of the CWT coefficient.

Fig.22 (a-1) shows the 3D plot of the average of the difference of the CWT coefficient of the two signal series s_1 and s_2 obtained from the first four interpolated mode shape data of the cracked aluminum beam. The corresponding contour plot of the average of the difference of the CWT coefficient is shown in Fig. 22 (a-2). The figures show very clear evidences of crack existence at 400 mm from the left end.

Similarly, the denoising results are shown in Fig.22 (b-1) and (b-2), which are the 3D plot of the average of the difference of the CWT coefficient, and the corresponding

contour plot. It follows clearly that the crack is located at $l_c = 400\,mm$. These experimental results therefore verify the efficiency and practicability of the proposed method. It is also noted that the computational time of the proposed method based on CWT coefficient difference is less than 200 ms and therefore the speed of processing of experimental data is not an issue. Furthermore, the procedure can be easily made automatic using Matlab wavelet and signal processing toolboxes, so the proposed method can be recommended for real monitoring applications.

7. Concluding remarks

This paper proposes a new approach based on the difference of the CWT coefficients of the two reconstructed signal series to provide a method without baseline modal parameters for damage detection in beam-like structures with small cracks, whose crack ratio ($r = H_c / H$) is less than 5%. The two signal series are obtained and reconstructed from the original mode shape 'signal' of a cracked beam. For a beam containing a single crack, one of these 'signals', which is apparently a smooth curve, actually exhibits a local peak or discontinuity in the region of damage because it includes additional response due to the crack.

The modal responses of the damaged simply-supported beams used were computed using the finite element method. Different crack locations and sampling distances were studied. The results demonstrate the efficiency of the proposed method for crack detection, and they also provide a better crack indicator than the result of the CWT of the original mode shape 'signal'. The simulated results show that the proposed method has great potential in crack detection of beam-like structures.

Experimental tests using a simply-supported aluminum beam were also conducted in the present work. In order to improve the accuracy of the crack detection, a spline interpolation was applied to each set of the measured data points for the first four mode shapes. The average of the difference of the CWT coefficient of all modes, is used as damage index for small crack detection in real applications. The experimental results demonstrate the precision and practicability of the proposed method, which can be recommended for real applications even when the crack is in the early state.

It should be noted that the use of this method based on CWT requires fairly accurate estimates of the mode shapes. This is the difficulty for application to real structures. Generally, to get accurate estimates of the mode shapes, however, one needs detailed measurements of the mode shapes. This fact increases considerably the duration of the investigation and this is the main disadvantage of using mode shapes for crack identification. However, with the availability of fast measurement techniques, such as scanning laser vibrometer [30], this limitation is not a serious issue. On the other hand, it has been shown that less detailed measurement can still be used provided that a spline interpolation is used to improve the accuracy of the crack detection.

Appendix A. Nomenclature

l_c	crack location of cracked beam from the left support
l	length of beams
b	width of beams
H	depth of beams
H_c	crack depth of beams
W_c	crack width of beams
E	Young's modulus of material
ρ	density of material
ν	Poisson ratio of material
L_e	element length
r	crack ratio
$\psi(x)$	mother wavelet function
$F_\psi(\omega)$	Fourier transform of $\psi(x)$
s	dilation parameter
b	translation parameter
$f(x)$	analyzed signal
$F_f(\omega)$	Fourier transform of $f(x)$

$(W_f)(s,b)$	Continuous wavelet transform of $f(x)$
Δx_ψ	duration of the mother wavelet of $\psi(x)$
$\Delta\omega_\psi$	bandwidth of the mother wavelet of $\psi(x)$
Δx	local resolution of the CWT in time or space
$\Delta\omega$	local resolution of the CWT in frequency
x_ψ	the centre of $\psi(x)$
ω_ψ	the centre of $F_\psi(\omega)$
$\|\cdot\|_2$	the classical norm in the space of square integrable functions

References

[1] Pandey, A.K., Biswas, M., Samman, M.M., Damage detection from changes in curvature mode shapes, Journal of Sound and Vibration145 (2) (1991), pp.321-332

[2] Ratcliffe, C. P., Damage detection using a modified Laplacian operator on mode shape data", Journal of Sound and Vibration 204 (1997), pp.505-517

[3] Zhong, S., Oyadiji, S. O, "Damage detection in simply supported beams using derivatives of mode shapes", Twelfth International Congress on Sound and Vibration, Lisbon, Portugal (2005), pp.11-14

[4] M.M. Abdel Wahab, Guido De Roeck, Damage detection in bridges using modal curvatures: application to a real damage scenario, Journal of Sound and Vibration 226(2) (1999), pp.217-235

[5] R.P.C. Sampaio, N.M.M. Maia, J.M.M. Silva, Damage detection using the frequency-response-function curvature method, Journal of Sound and Vibration 226 (5) (1999), pp. 1029 – 1042[6] Peng, Z.K., Chu, F.L., Application of the wavelet transform in machine condition monitoring and fault diagnostics: a review with bibliography, Mechanical Systems and Signal Processing 18 (2004), pp.199 – 221.

[7] Deng, X., Wang, Q., Crack detection using spatial measurements and wavelet, International Journal of Fracture 91 (1998), pp.23-28.

[8] Tian, J.Y., Li, Z., Su, X.Y., "Crack detection in beams by wavelet analysis of transient flexural waves", Journal of Sound and Vibration 261 (2003), pp.715-727

[9] Wang, Q., Deng, X., Damage detection with spatial wavelets, International Journal of Solids and Structures 36 (1999), pp.3443-3468.

[10] Liew, K.M., Wang, Q., Application of wavelet theory for crack identification in structures, Journal of Engineering Mechanics 124 (1998), 152-157.

[11] Gentile, A., Messina, A., On the continuous wavelet transforms applied to discrete vibrational data for detecting open cracks in damaged beams, International Journal of Solids and Structrues 40 (2003), pp.295-315.

[12] Quek, S. T., Wang, Q., Zhang, L., K. Ang, Sensitivity analysis of crack detection in beams by wavelet technique, International Journal of Mechanical Sciences 43(12) (2001), pp.2899-2910.

[13] Hong, J. C., Kim, Y. Y., Lee, H. C., Lee, Y. W., Damage detection using the Lipschitz exponent estimated by the wavelet transform: applications to vibration modes

of a beam, International Journal of Solids and Structures 39 (2002), pp.1803-1816.

[14] Yan, Y.J., Hao, H.N., Yam, L.H., Vibration-based construction and extraction of structural damage feature index, International Journal of Solids and Structures 41 (2004), pp.6661-6676.

[15] Douka, E., Loutridis, S., Trochidis, A., "Crack identification in beams using wavelet analysis", International Journal of Solids and Structure 40 (2003), pp.3557-3569

[16] Han, J. G, Ren, W. X., Sun, Z. S., Wavelet packet based damage identification of beam structures, International Journal of Solids and Structures 42 (2005), pp.6610-6627.

[17] Chang, C. C., Chen, L. W., Detection of the location and size of cracks in the multiple cracked beam by spatial wavelet based approach, Mechanical Systems and Signal Processing 19 (2005), pp.139-155.

[18] Zumpano, G. and Meo, M., A new damage detection technique based on wave propagation for rails, International Journal of Solids and Structures 43 (2006), pp.1023-1046.

[19] Kim, B. H., Taehyo Park, T., Voyiadjis, G. Z., Damage estimation on beam-like structures using the multi-resolution analysis, International of Solids and Structures 43 (2006), pp.14-15.

[20] Zhu, X.Q., Law, S.S., Wavelet-based crack identification of bridge beam from operational deflection time history, International Journal Solids and Structures 43 (2006), pp.2299-2317.

[21] Daubechies, I., Ten lectures on wavelets, Society for Industrial and Applied Mathematics, Philadelphia, PA, USA (1992).

[22] Haase, M., Widjajakusuma, J., Damage identification based on ridges and maxima lines of the wavelet transform, International Journal of Engineering Science 41 (2003), pp.1423-1443.

[23] Le, T. P., Argoul, P., Continuous wavelet transform for modal identification using free decay response, Journal of Sound and Vibration 277 (2004), pp.733-100.

[24] Skopina, M., On construction of multivariate wavelets with vanishing moment, Applied and Computational Harmonic Analysis 20 (2006), pp.375-390.

[25] Qiao, P, Cao, M, Waveform fractal dimension for mode shape-based damage identification of beam-type structures, International identification of beam-type structures 45 (2008), pp. 5946-5961.

[26] Farrar, C.R, Doebling, S.W., An overview of modal-based damage identification methods. In: EUROMECH 365 International Workshop: DAMAS 97, Structural Damage Assessment Using Advanced Signal Processing Procedures, Sheffield, UK.

[27] Zhong, S., Oyadiji, S. O, "Crack Detection in Simply-Supported Beams without Baseline Modal Parameters by Stationary Wavelet Transform", Mechanical Systems and Signal Processing, 21 (2007), pp1853–1884

[28] Zhong, S., Oyadiji, S. O, "Identification of Cracks in Beams with Auxiliary Mass Spatial Probing by Stationary Wavelet Transform", ASME Journal of Vibration and Acoustics, 130 (2008), 041001:1-14.

[29] Zhong, S., Oyadiji, S. O, "Crack Detection in Simply Supported Beams Using Stationary

Wavelet Transform of Modal Data", Structural Control and Health Monitoring (accepted), (2009), DOI: 10.1002/stc.366

[30] J. Vanherzeele, S. Vanlanduit and P. Guillaume, "Reducing measurement time for a laser Doppler vibrometer using regressive techniques", Optics and Lasers in Engineering, 45(1) 2007, pp 49-56.

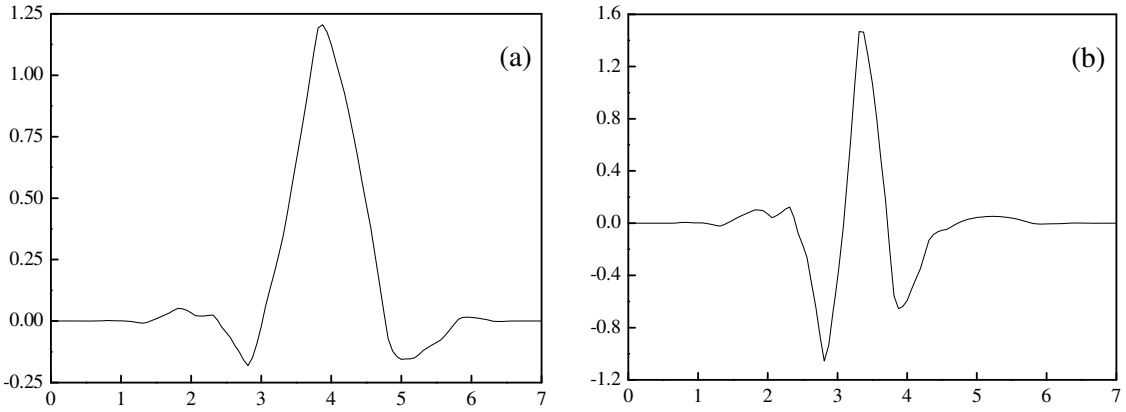

Fig.1. 'Symmetrical 4' wavelet: (a) Scaling function, (b) Wavelet function (mother wavelet)

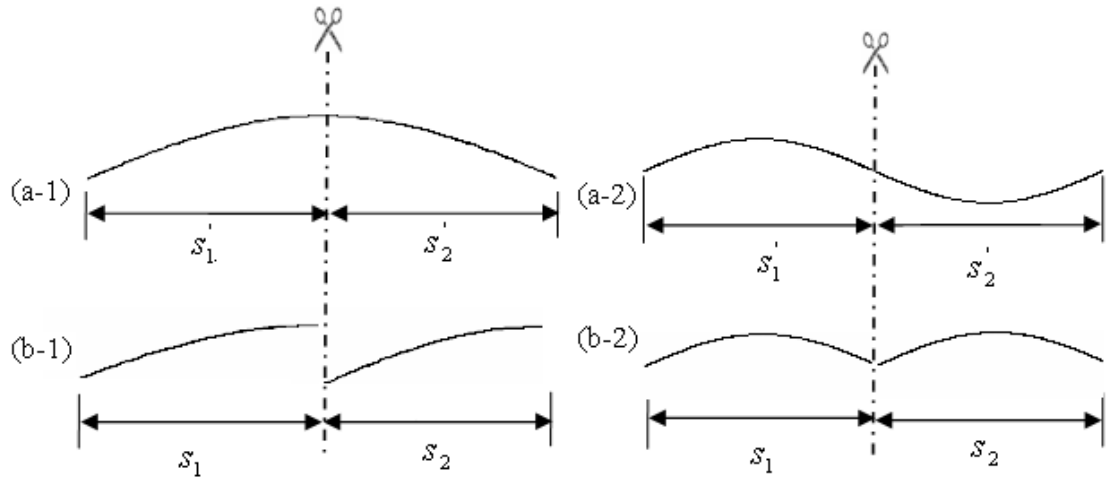

Fig.2 Two series signals divided and reconstructed from the original mode shape data

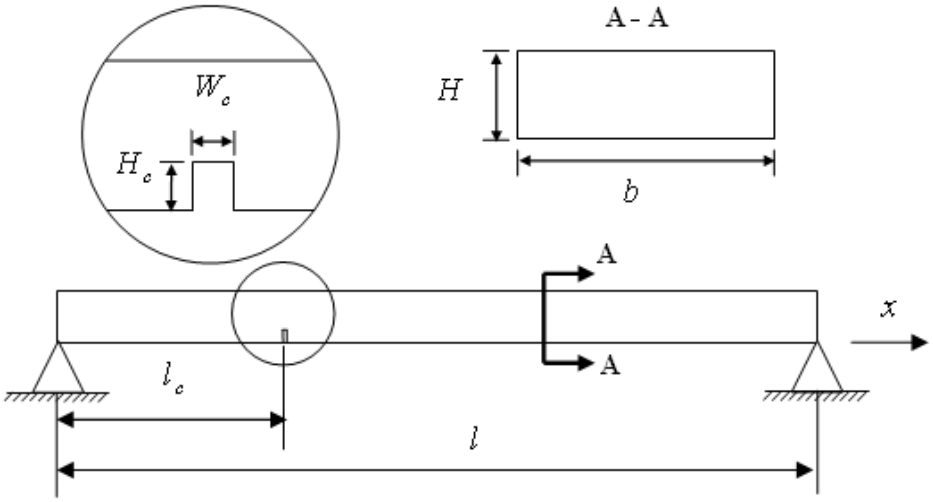

Fig.3 Model of cracked simply-supported beam

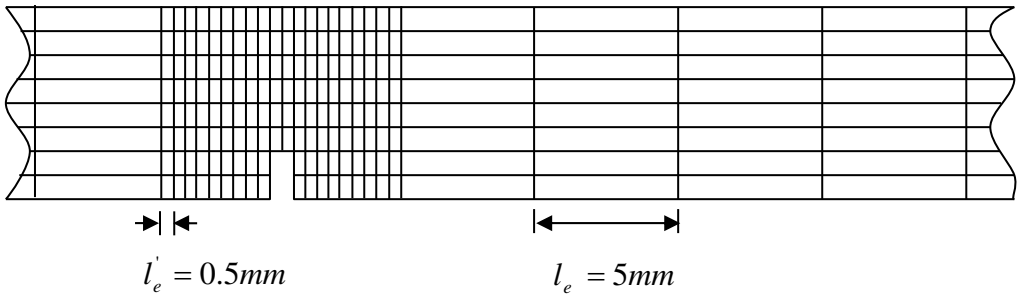

Fig.4 Side view of FE mesh around cracked region

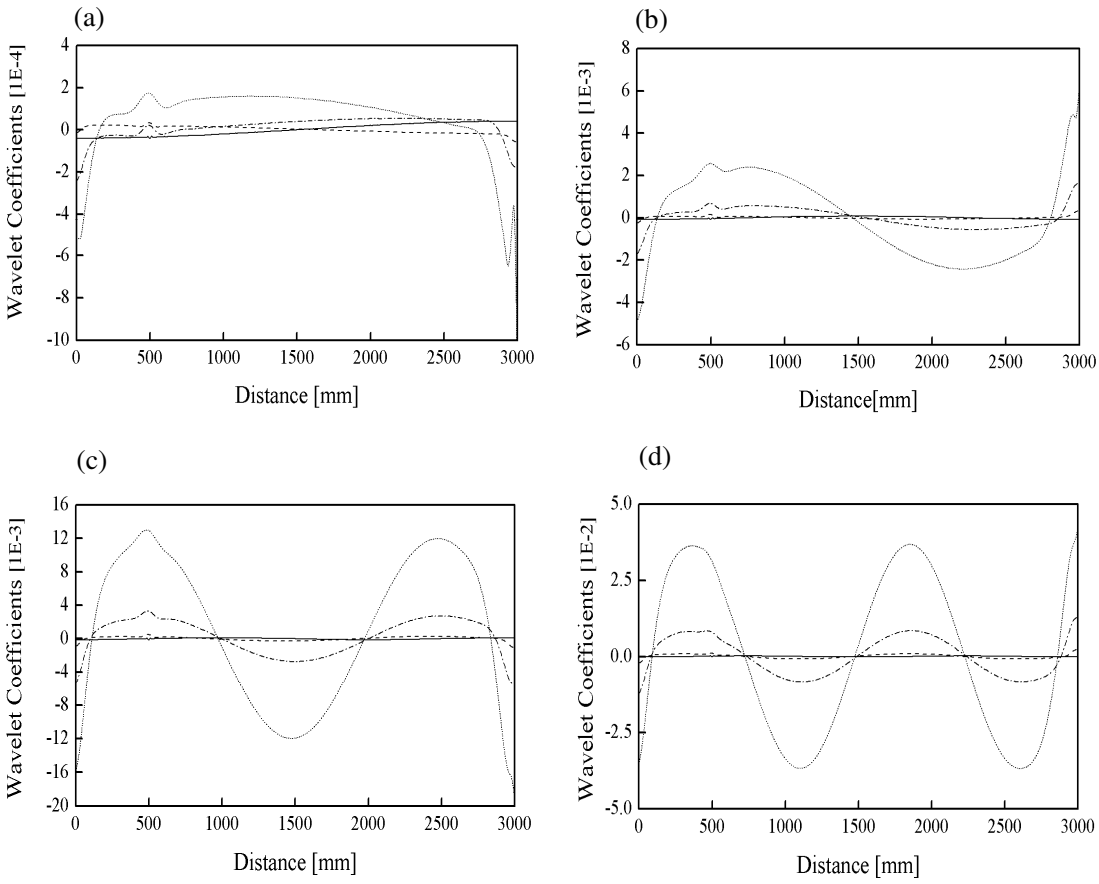

Fig.5 CWT coefficients of the original mode shapes for different scales: $W_c = 0.1\,mm$, $H_c = 1\,mm$, $x_s = 5\,mm$, $l_c = 500\,mm$, ——— scale = 5, - - - - scale =15, -·-·-· scale = 25, ····· scale = 35, (a) mode 1, (b) mode 2, (c) mode 3, and (d) mode 4

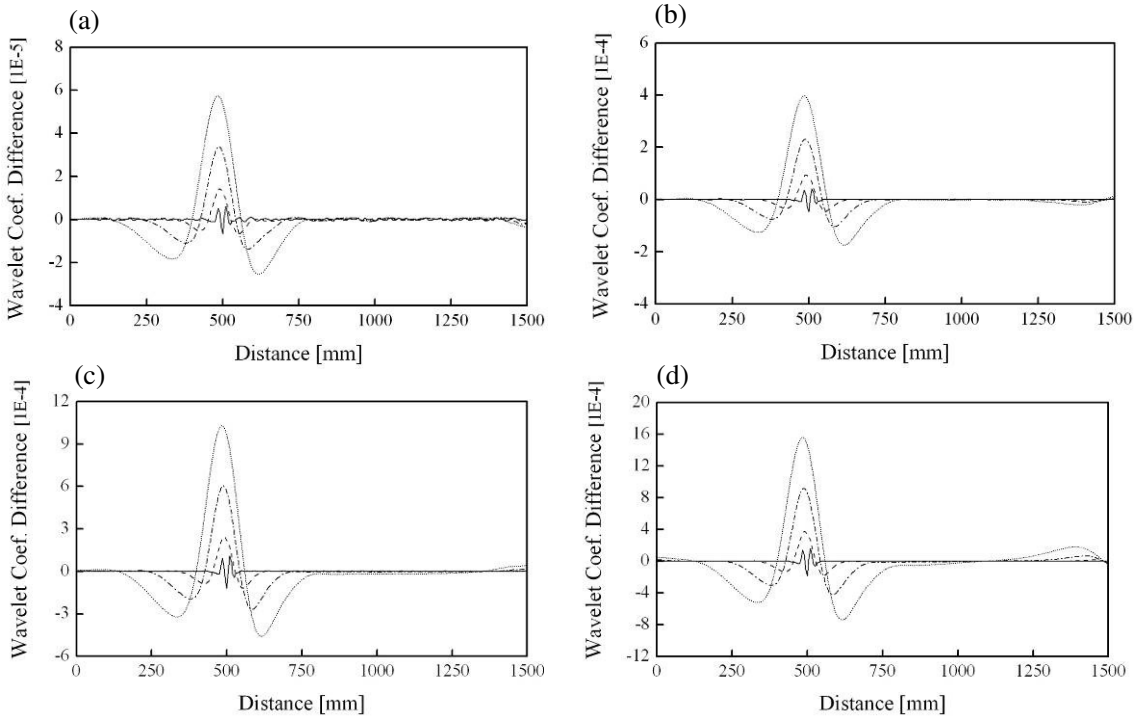

Fig.6 The difference of the CWT coefficients of s_1 and s_2 for different scales: $W_c = 0.1\,mm$, $H_c = 1\,mm$, $x_s = 5\,mm$, $l_c = 500\,mm$, ——— scale = 5, - - - - scale =15, -·-·-·- scale = 25, ····· scale = 35, (a) mode 1, (b) mode 2, (c) mode 3, and (d) mode 4

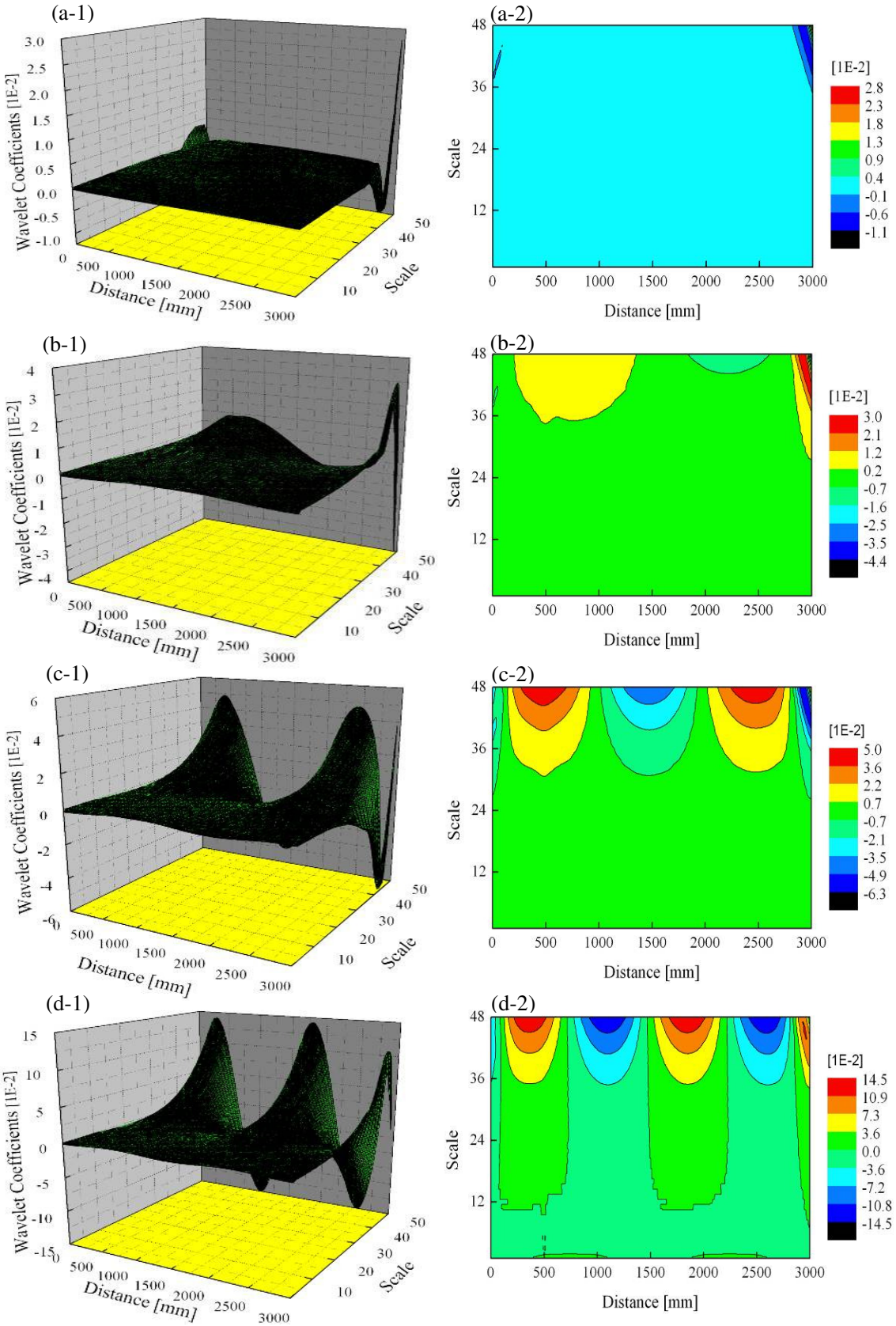

Fig.7 3D (left) and contour (right) plots of the CWT of the original mode shapes showing the trend of the wavelet modulus maxima for (a) mode 1, (b) mode 2, (c) mode 3, and (d) mode 4; $W_c = 0.1\,mm$, $H_c = 1\,mm$, $x_s = 5\,mm$ $l_c = 500\,mm$

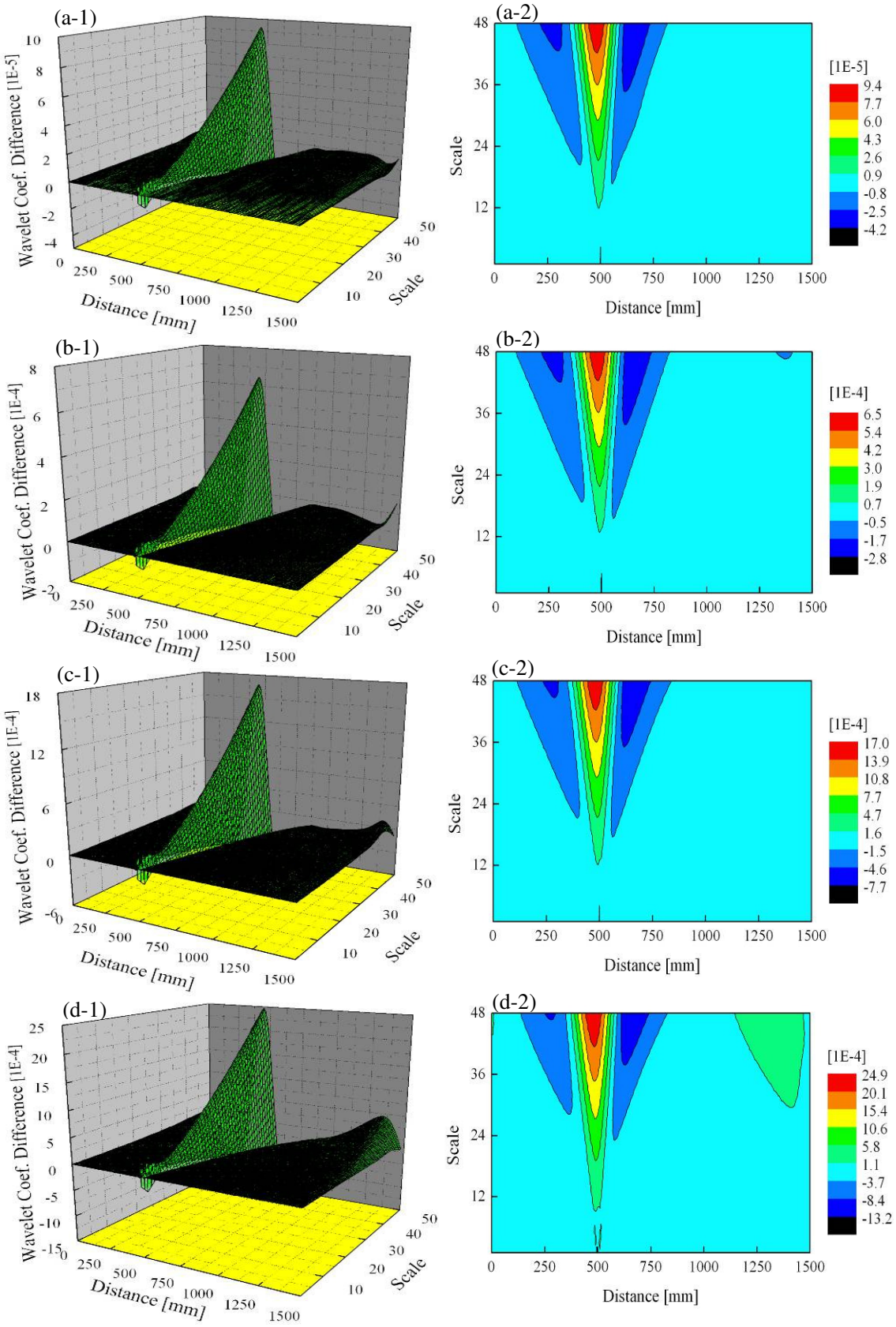

Fig.8 3D (left) and contour (right) plots of the difference of the CWT coefficients of s_1 and s_2 showing the trend of the modified wavelet modulus maxima for (a) mode 1, (b) mode 2, (c) mode 3, and (d) mode 4; $W_c = 0.1\,mm$, $H_c = 1\,mm$, $x_s = 5\,mm$ $l_c = 500\,mm$

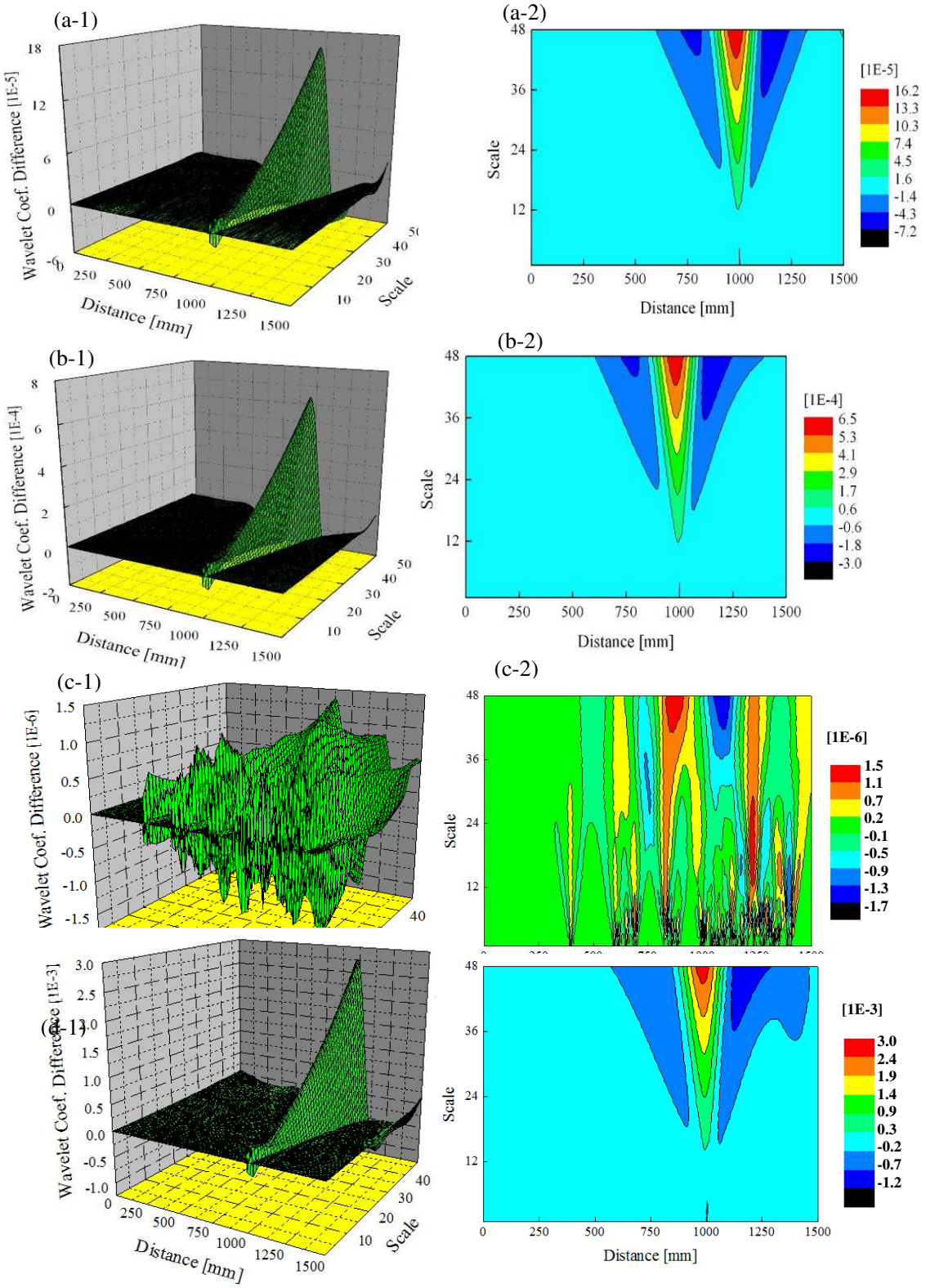

Fig.9 3D (left) and contour (right) plots of the difference of the CWT coefficients of s_1 and s_2 showing the trend of the wavelet modulus maxima for (a) mode 1, (b) mode 2, (c) mode 3 and (d) mode 4; $W_c = 0.1\,mm$, $H_c = 1\,mm$, $x_s = 5\,mm$, $l_c = 1000\,mm$

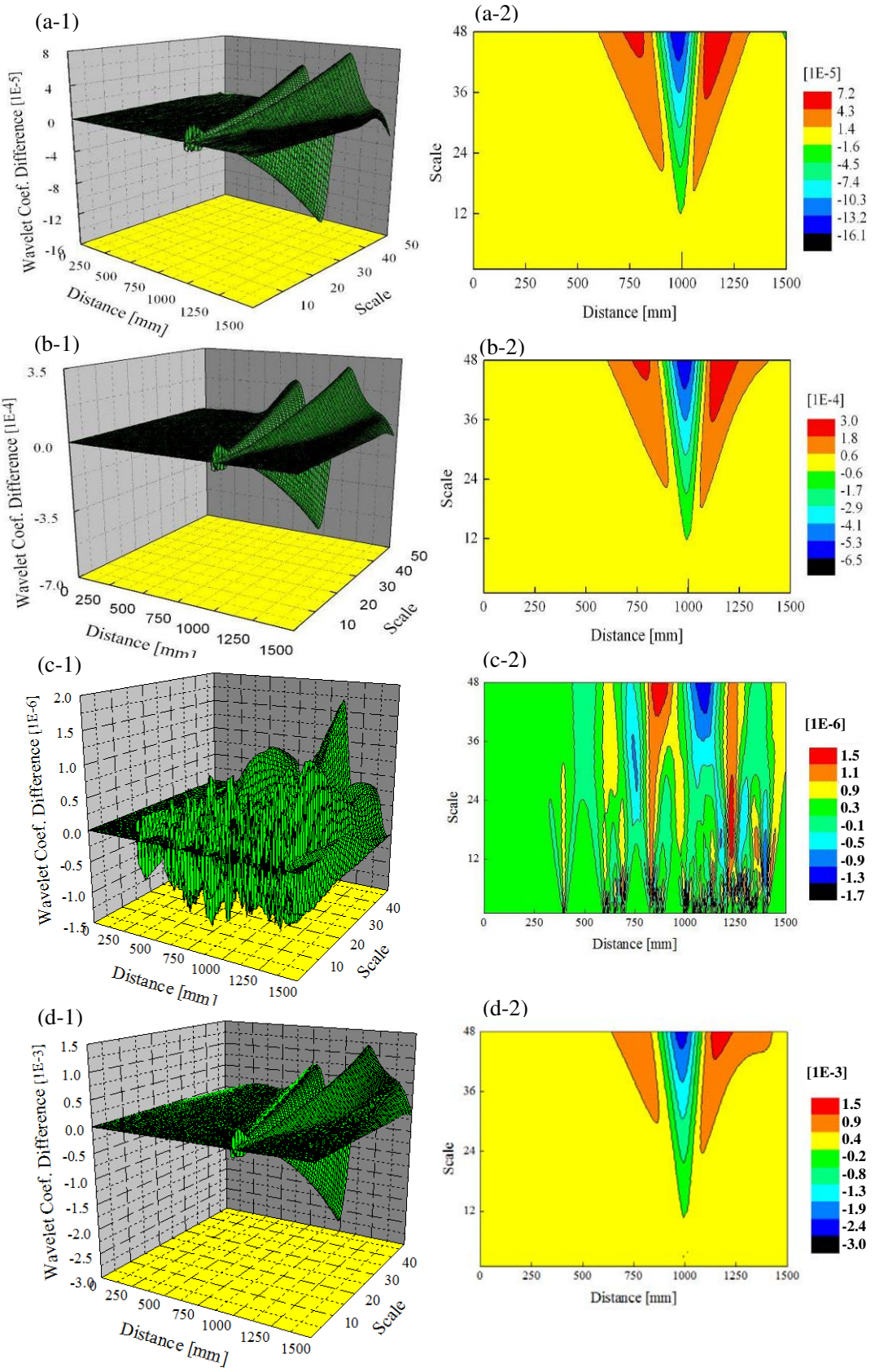

Fig.10 3D (left) and contour (right) plots of the difference of the CWT coefficients of s_1 and s_2 showing the trend of the wavelet modulus maxima for (a) mode 1, (b) mode 2, (c) mode 3 and (d) mode 4; $W_c = 0.1\,mm$, $H_c = 1\,mm$, $x_s = 5\,mm$, $l_c = 2000\,mm$

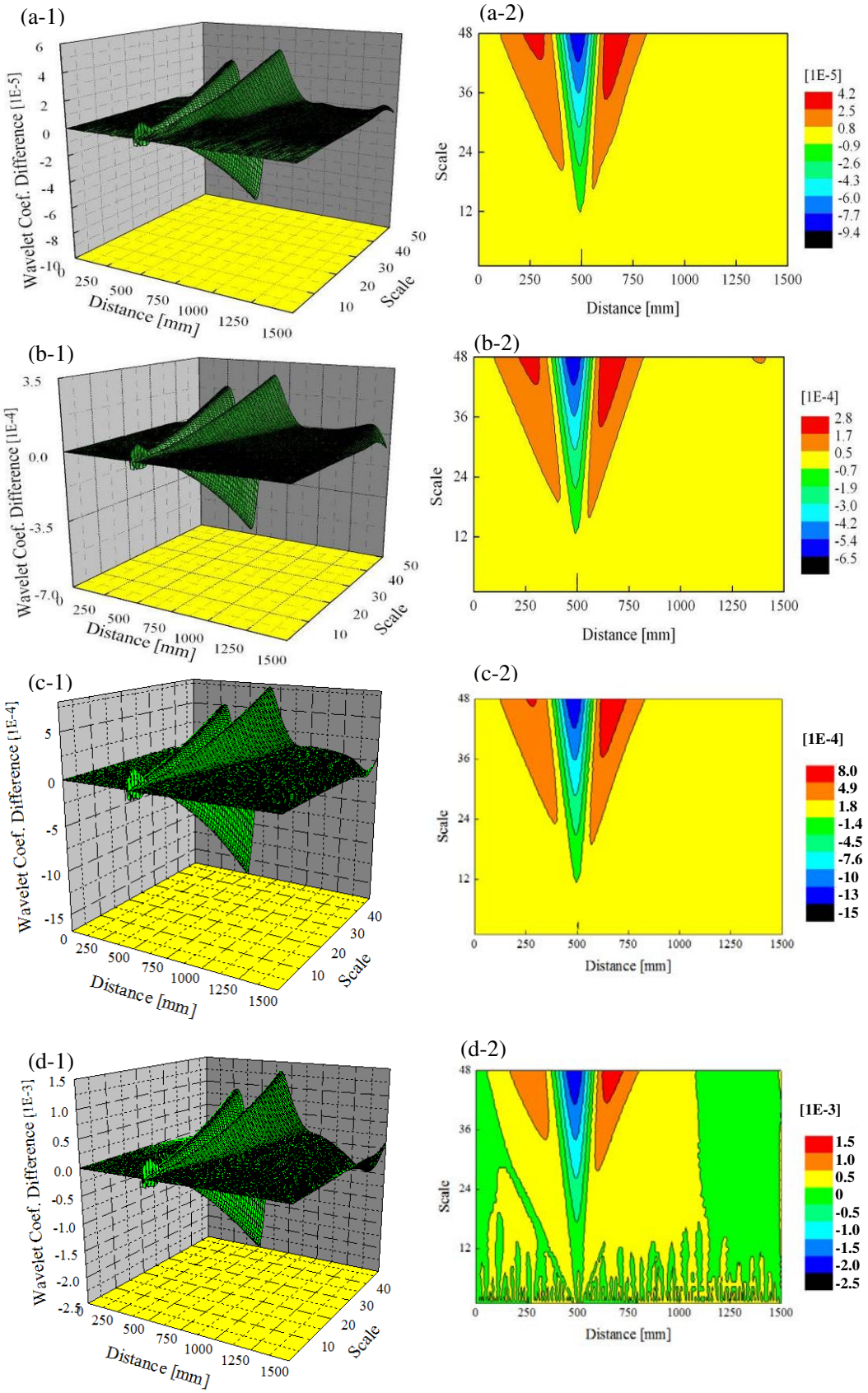

Fig.11 3D (left) and contour (right) plots of the difference of the CWT coefficients of s_1 and s_2 showing the trend of the wavelet modulus maxima for (a) mode 1, (b) mode 2, (c) mode 3, and (d) mode 4; $W_c = 0.1\,mm$, $H_c = 1\,mm$, $x_s = 5\,mm$, $l_c = 2500\,mm$

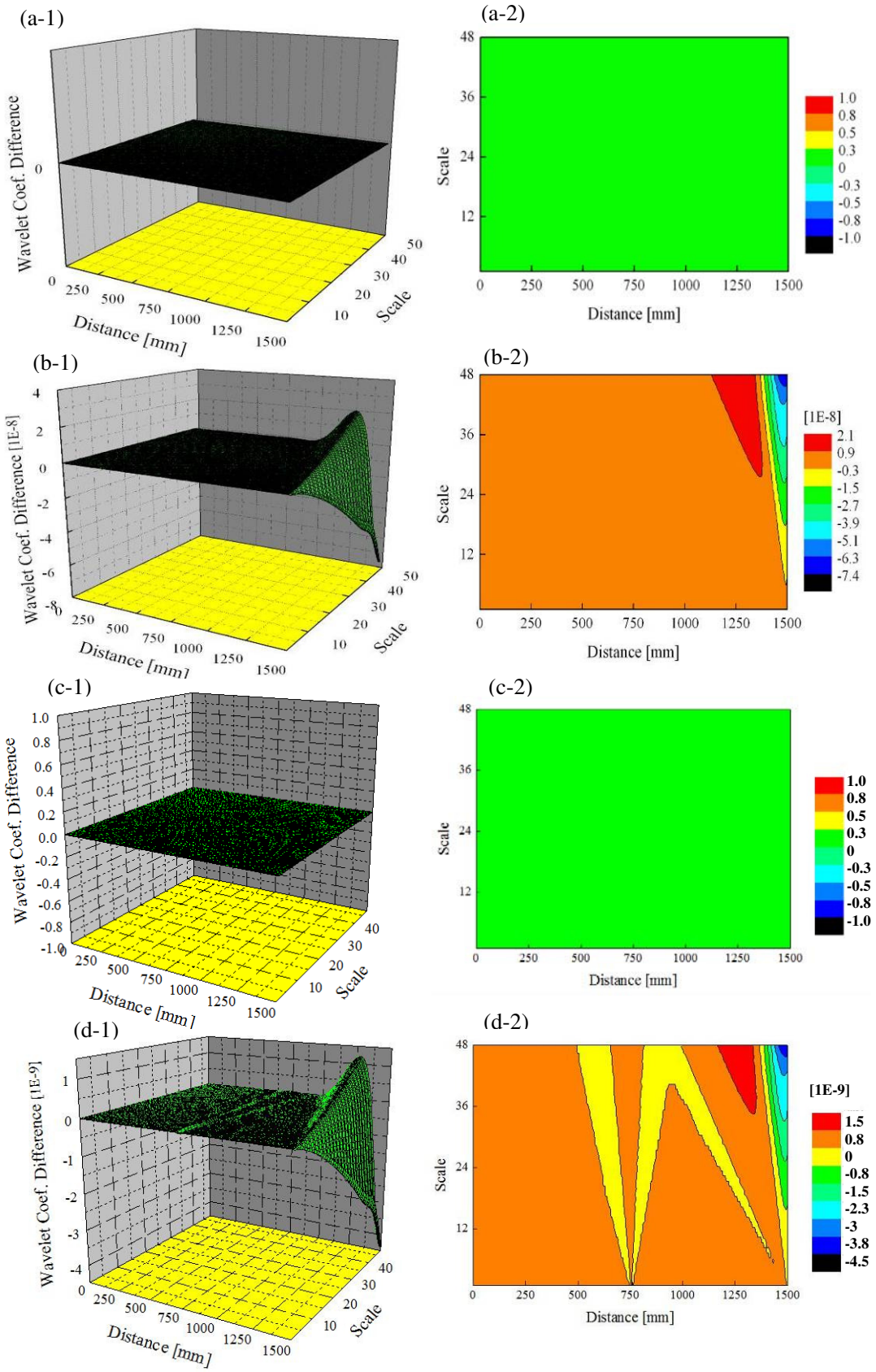

Fig.12 3D (left) and contour (right) plots of the difference of the CWT coefficients of s_1 and s_2 showing the trend of the wavelet modulus maxima for (a) mode 1, (b) mode 2, (c) mode 3, and (d) mode 4; $W_c = 0.1\,mm$, $H_c = 1\,mm$, $x_s = 5\,mm$, $l_c = 1500\,mm$

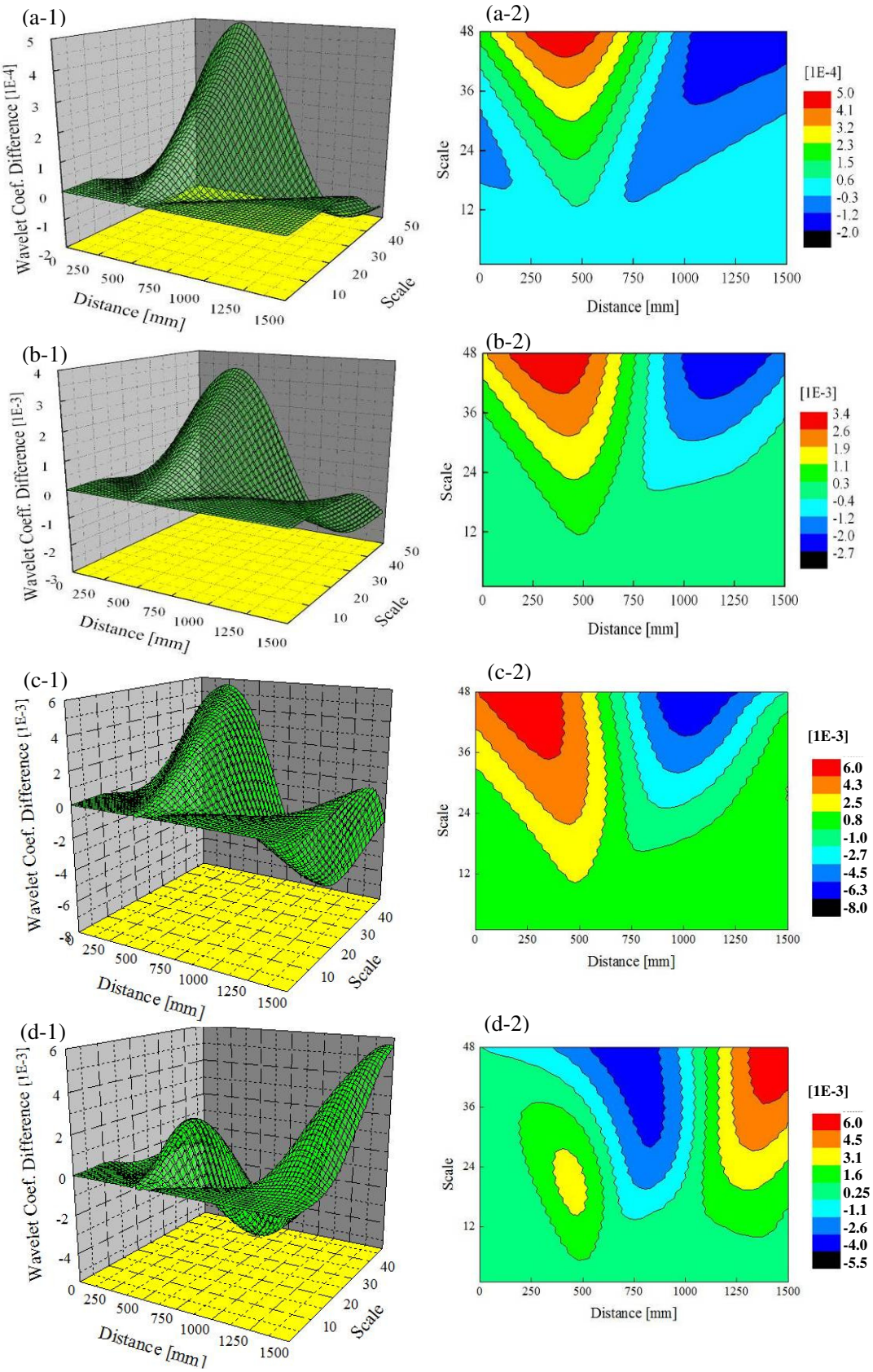

Fig.13 3D (left) and contour (right) plots of the difference of the CWT coefficients of s_1 and s_2 showing the trend of the wavelet modulus maxima for sampling distance $x_s = 25\ mm$: (a) mode 1, (b) mode 2, (c) mode 3 and (d) mode 4; $W_c = 0.1\ mm$, $H_c = 1\ mm$, $l_c = 500\ mm$

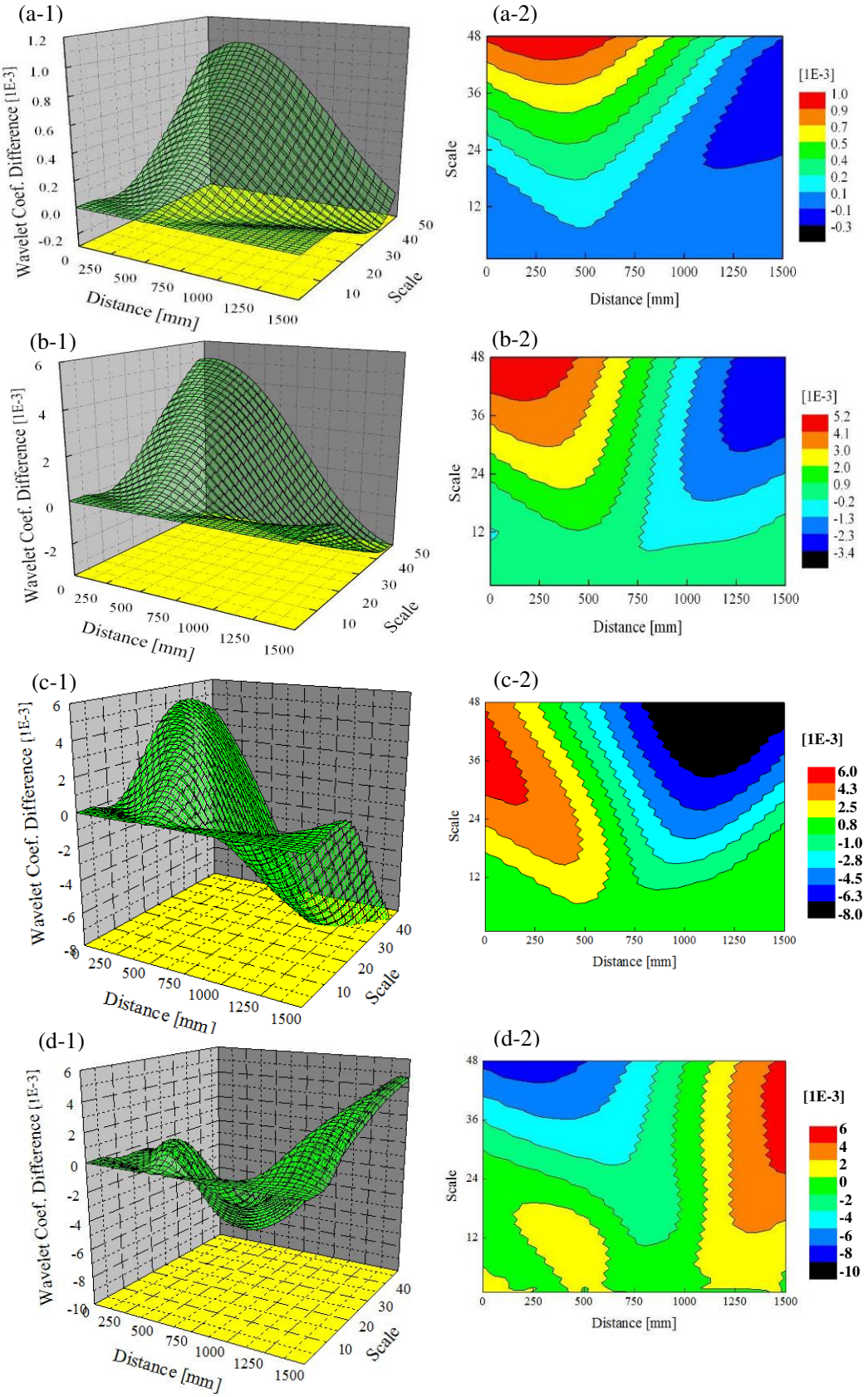

Fig.14 3D (left) and contour (right) plots of the difference of the CWT coefficients of s_1 and s_2 showing the trend of the wavelet modulus maxima for sampling distance $x_s = 50\ mm$: (a) mode 1, (b) mode 2, (c) mode 3 and (d) mode 4; $W_c = 0.1\ mm$, $H_c = 1\ mm$, $l_c = 500\ mm$

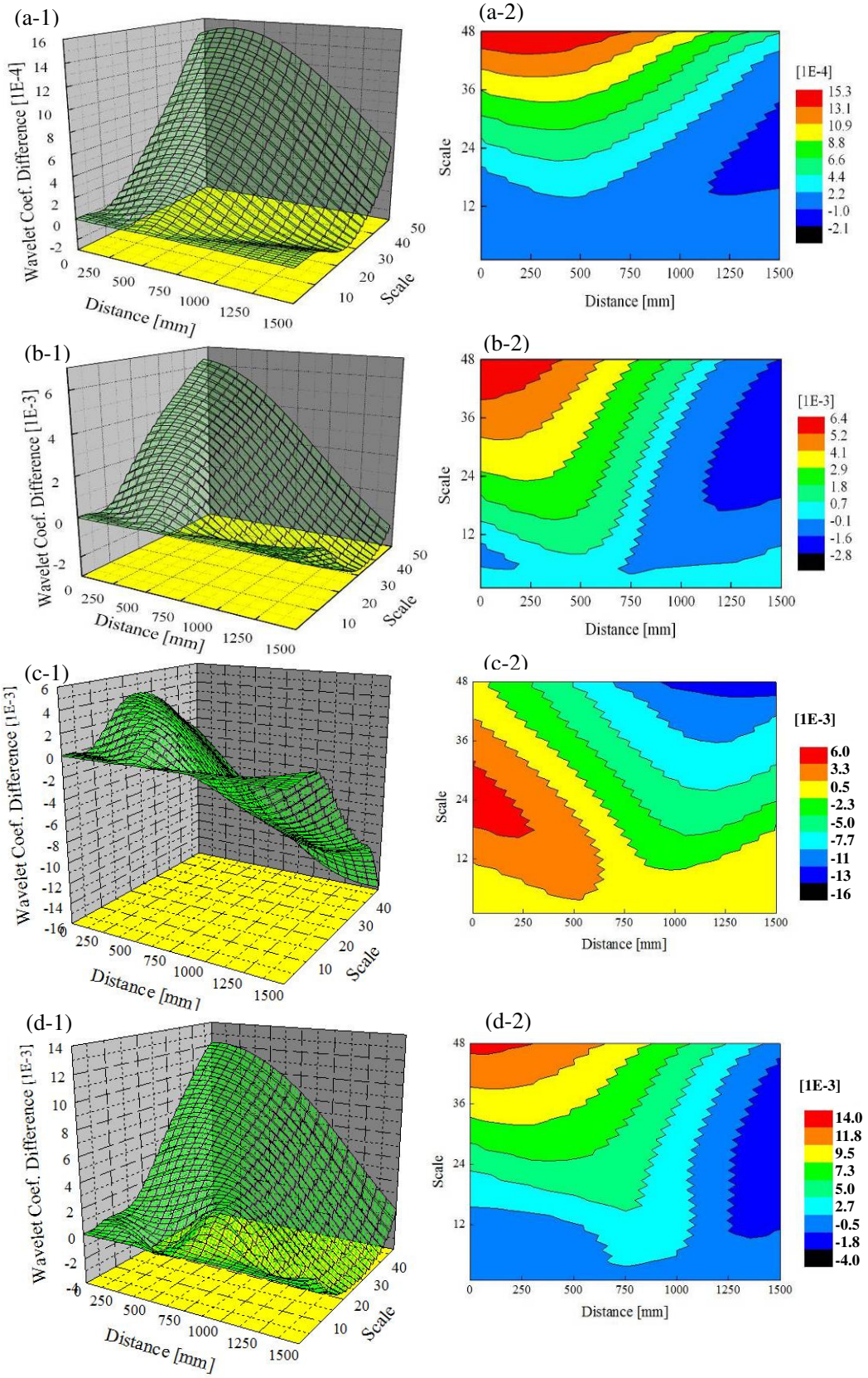

Fig.15 3D (left) and contour (right) plots of the difference of the CWT coefficients of s_1 and s_2 showing the trend of the wavelet modulus maxima for sampling distance $x_s = 75\ mm$ (a) mode 1, (b) mode 2, (c) mode 3 and (d) mode 4; $W_c = 0.1\ mm$, $H_c = 1\ mm$, $l_c = 500\ mm$

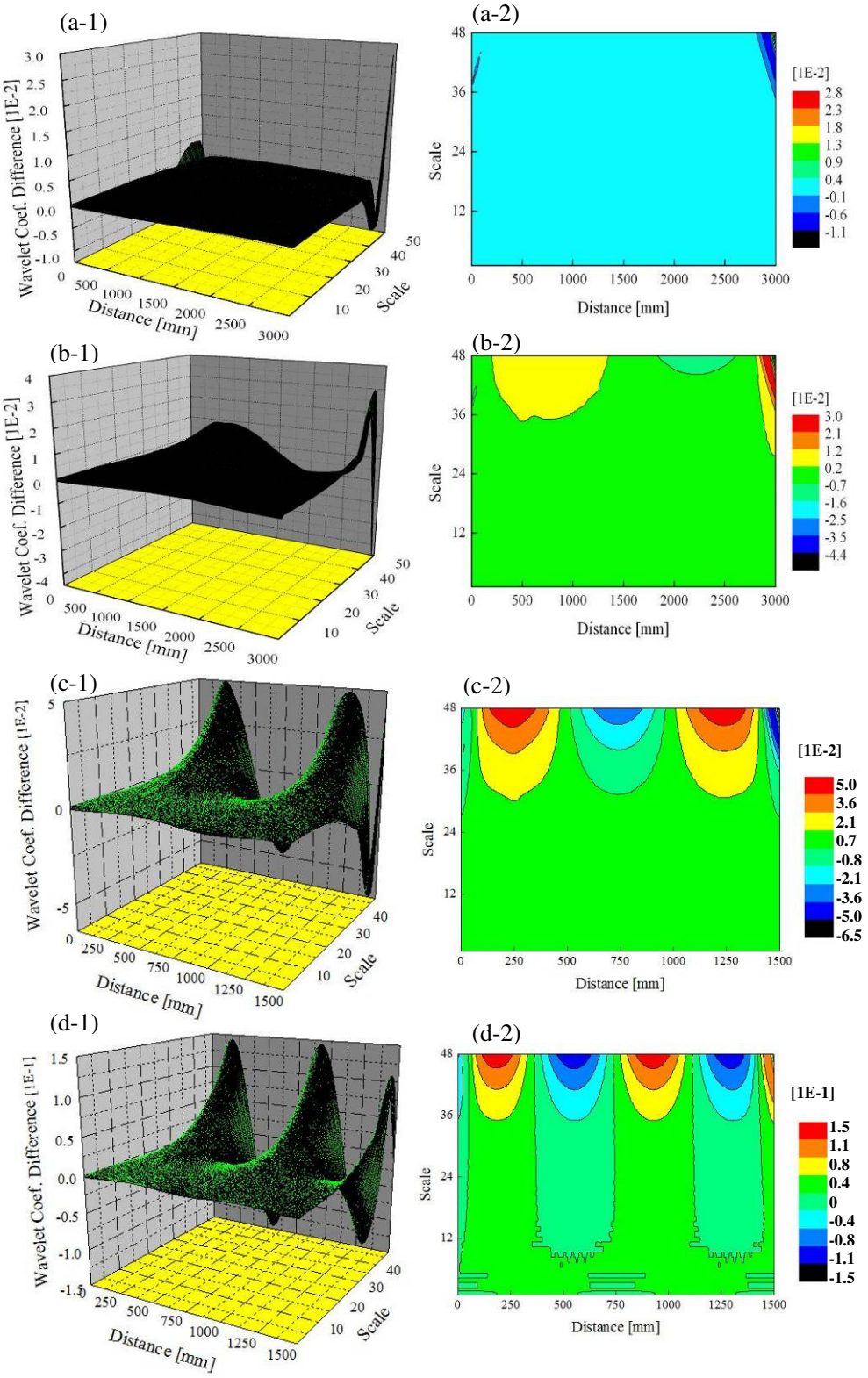

Fig.16 3D (left) and contour (right) plots of the CWT of the interpolated original mode shapes showing the trend of the wavelet modulus maxima for sampling distance $x_s = 75\ mm$: (a) mode 1, (b) mode 2, (c) mode 3 and (d) mode 4; $W_c = 0.1\ mm$, $H_c = 1\ mm$, $l_c = 500\ mm$

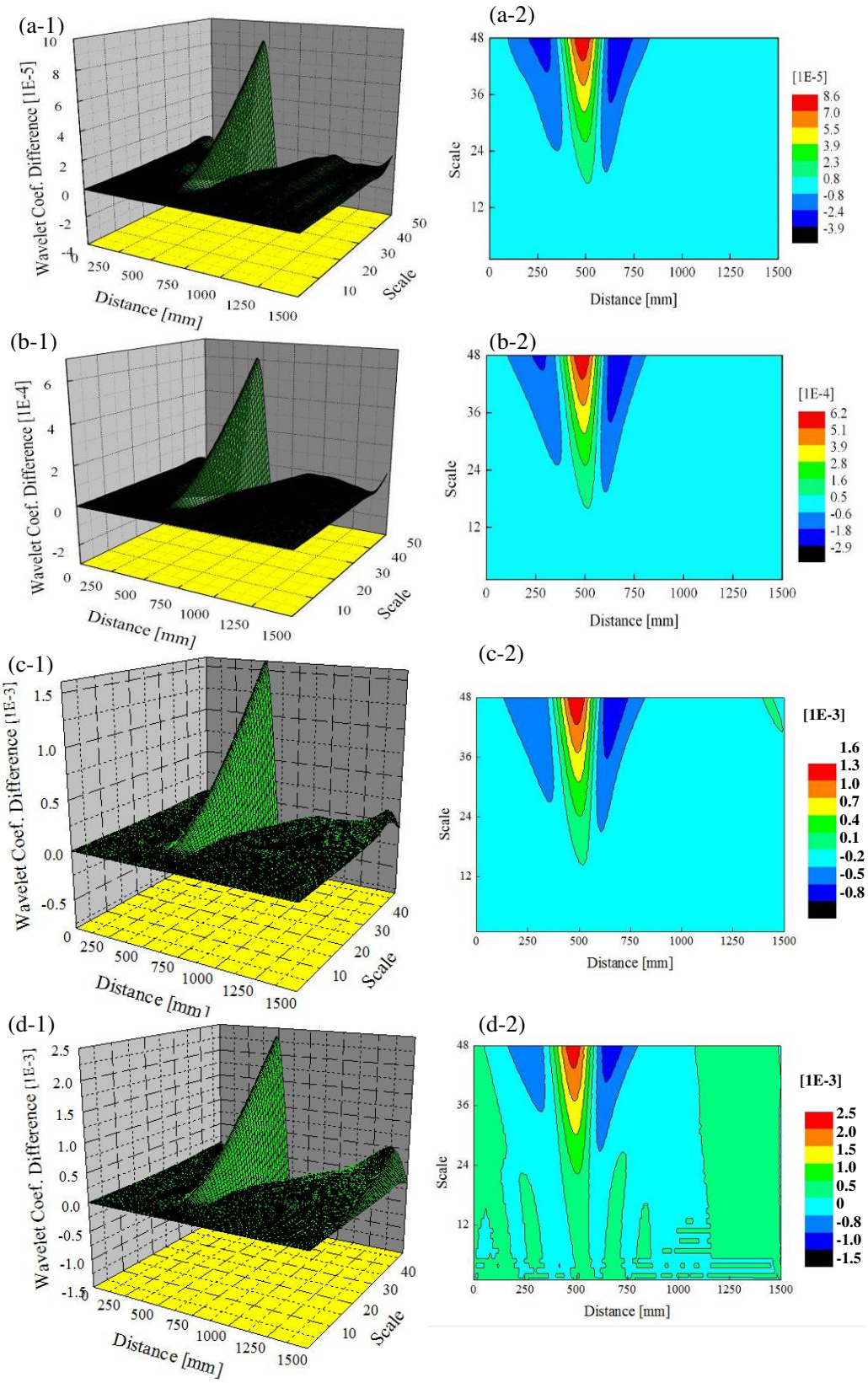

Fig.17 3D (left) and contour (right) plots of the difference of the CWT coefficients of s_1 and s_2 obtained from the first two interpolated mode shapes showing the trend of the wavelet modulus maxima for (a) mode 1, (b) mode 2, (c) mode 3 and (d) mode 4; $W_c = 0.1\,mm$, $H_c = 1\,mm$, $x_s = 75\,mm$, $l_c = 500\,mm$

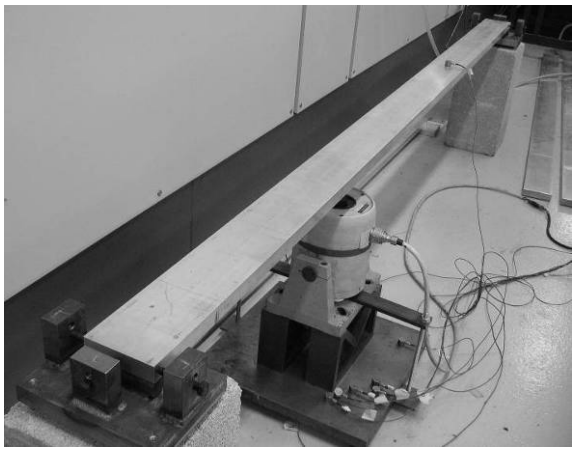

Fig.18 Experimental Setup

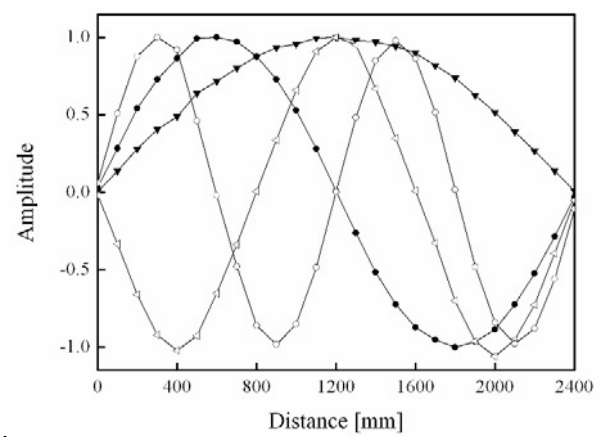

Fig.19 The first four measured mode shape of a cracked aluminum simply supported beam ($W_c = 1\,mm$ $H_c = 2.5mm$, $x_s = 100\,mm$, $l_c = 400\,mm$): mode 1, mode 2, mode 3, mode 4.

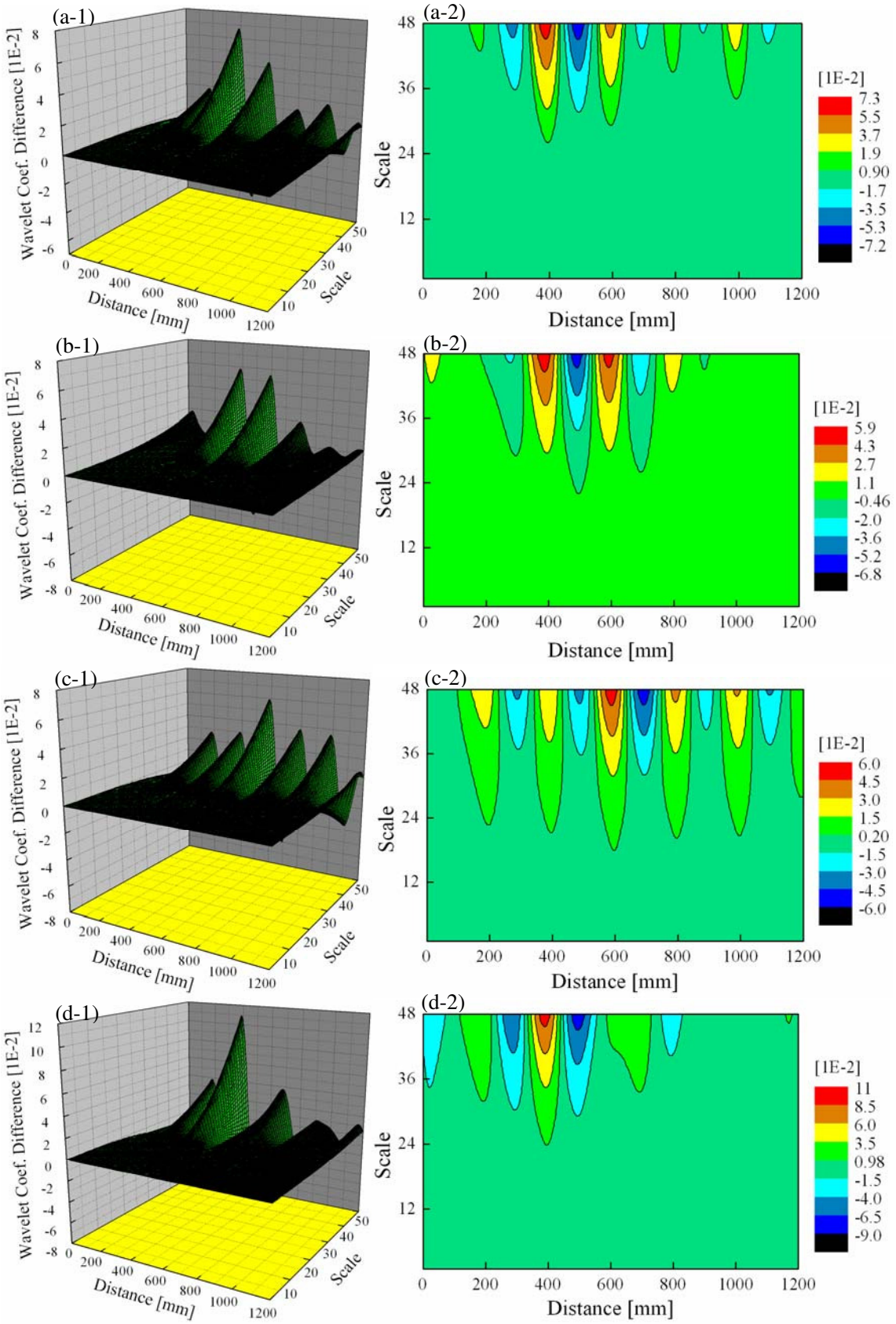

Fig.20 3D plots of CWT coefficient differences from the first four experimental mode shapes of an Aluminum beam showing the trend of the wavelet modulus maxima for (a) mode 1, (b) mode 2, (c) mode 3 and (d) mode 4; $W_c = 1\,mm$, $H_c = 2.5mm$, $x_s = 100\,mm$, $l_c = 400\,mm$

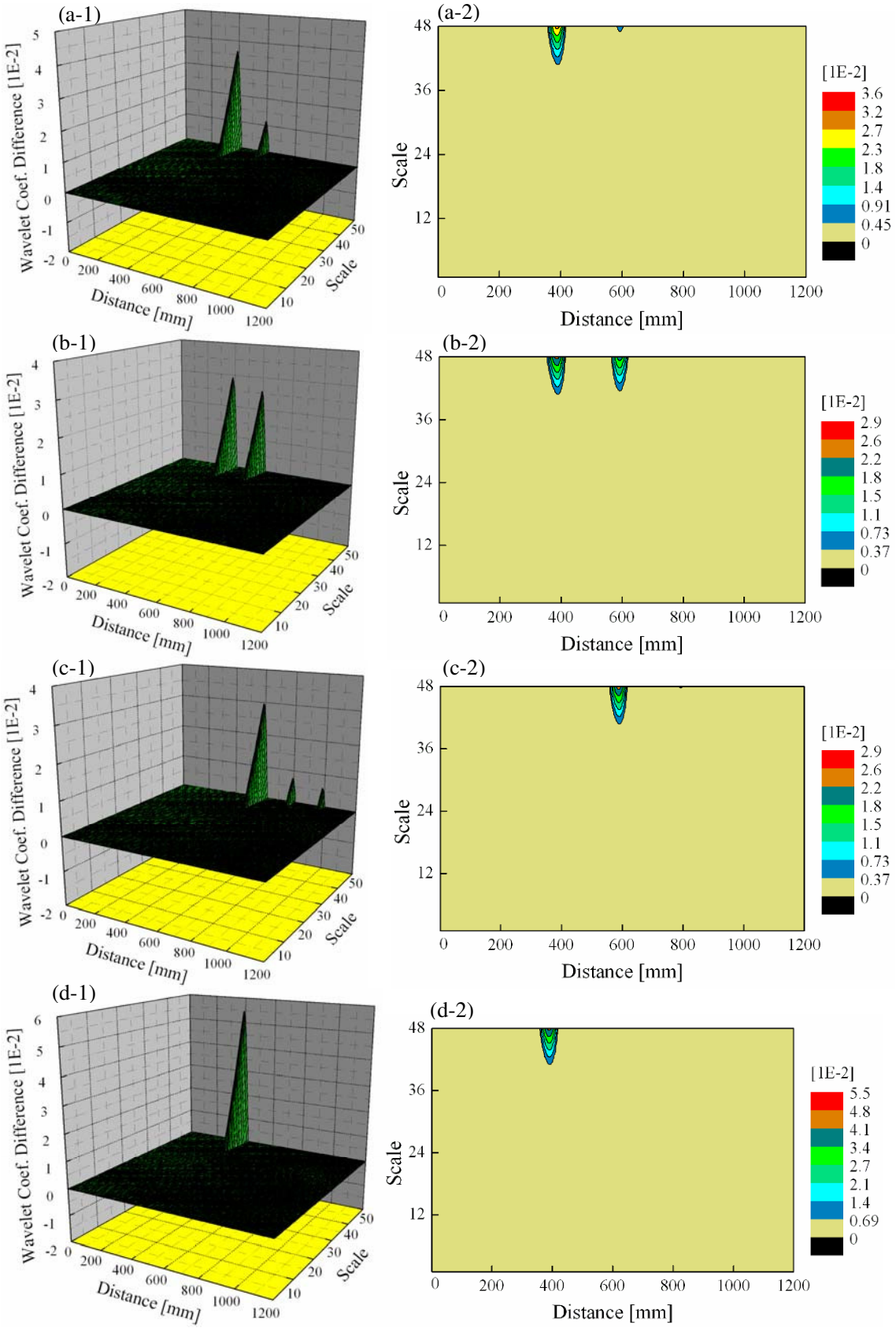

Fig.21 3D plots of denoised CWT coefficient differences from the first four experimental mode shapes of an Aluminum beam showing the trend of the wavelet modulus maxima for (a) mode 1, (b) mode 2, (c) mode 3 and (d) mode 4; $W_c = 1\,mm$, $H_c = 2.5mm$, $x_s = 100\,mm$, $l_c = 400\,mm$

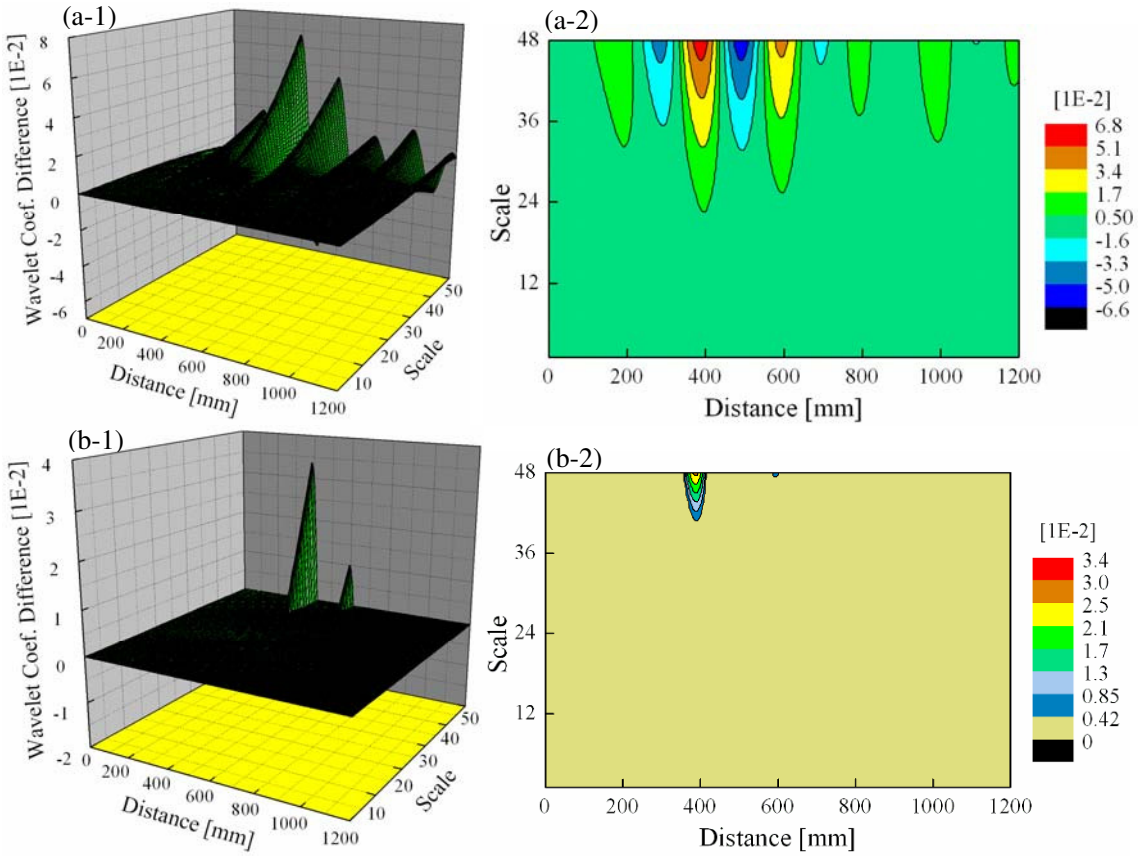

Fig.22 3D plots of the average of the CWT coefficient difference of s_1 and s_2 obtained from the first four experimental mode shapes of an aluminum beam showing the trend of the wavelet modulus maxima for (a) original data (b) denoised data; $W_c = 1\,mm$, $H_c = 2.5mm$, $x_s = 100\,mm$, $l_c = 400\,mm$

Table 1: Parameters of 15 cracked beams analysed: l_c is crack location, and x_s is the mode shape data sampling distance

$l_c(mm)$	$x_s(mm)$
500	5
1000	25
1500	50
2000	
2500	